https://doi.org/10.5194/acp-2020-1318
Preprint. Discussion started: 11 March 2021

Atmospheric Chemistry and Physics Discussions

Mid-latitude mixed-phase stratocumulus clouds and their interactions with aerosols: how ice processes affect microphysical, dynamic and thermodynamic development in those clouds and interactions?

Seoung Soo Lee[1,2], Kyung-Ja Ha[2], Manguttathil Gopalakrishnan Manoj[3], Mohammad Kamruzzaman[4,5], Hyungjun Kim[6], Nobuyuki Utsumi[7], Jianping Guo[8]

[1]Earth System Science Interdisciplinary Center, University of Maryland, College Park, Maryland, USA

[2]Department of Atmospheric Sciences, Division of Earth Environmental System, Pusan National University, Pusan, South Korea

[3]Advanced Centre for Atmospheric Radar Research, Cochin University of Science and Technology, Kerala, India

[4]School of Mathematical Sciences, University of Adelaide, Adelaide, Australia

[5]Natural and Built Environments Research Centre, Division of Information Technology, Engineering and the Environment (ITEE), University of South Australia, Adelaide,Australia

[6]Institute of Industrial Science, University of Tokyo, Tokyo, Japan

[7]Nagomori Institute of Actuators, Kyoto University of Advanced Science, Japan

[8]State Key Laboratory of Severe Weather, Chinese Academy of Meteorological Sciences, Beijing 100081, China

https://doi.org/10.5194/acp-2020-1318
Preprint. Discussion started: 11 March 2021

Atmospheric Chemistry and Physics Discussions

Corresponding author: Seoung Soo Lee
Office: (303) 497-6615
Cell: (609) 375-6685
Fax: (303) 497-5318
E-mail: cumulss@gmail.com, slee1247@umd.edu

https://doi.org/10.5194/acp-2020-1318
Preprint. Discussion started: 11 March 2021

Atmospheric Chemistry and Physics Discussions

Abstract

Mid-latitude mixed-phase stratocumulus clouds and their interactions with aerosols remain poorly understood. This study examines the roles of ice processes in those clouds and interactions using a large-eddy simulation (LES) framework. Cloud mass becomes much lower in the presence of ice processes and the Wegener-Bergeron-Findeisen (WBF) mechanism in the mixed-phase clouds as compared to that in warm clouds. This is because while the WBF mechanism enhances the evaporation of droplets, the low concentration of aerosols as ice nuclei (IN) and cloud ice number concentration (CINC) prevent the efficient deposition of water vapor whose mass is contributed by the evaporation. In the mixed-phase clouds, the increasing concentration of aerosols that act as cloud condensation nuclei (CCN) decreases cloud mass by increasing the evaporation of droplets through the WBF mechanism and decreasing the intensity of updrafts. In contrast to this, in the warm clouds, the absence of the WBF mechanism makes the increase in the evaporation of droplets inefficient, eventually enabling cloud mass to increase with the increasing concentration of aerosols as CCN. Here, the results show that when there is an increasing concentration of aerosols that act as IN, the deposition of water vapor is more efficient than when there is the increasing concentration of aerosols as CCN, which in turn enables cloud mass to increase in the mixed-phase clouds.

https://doi.org/10.5194/acp-2020-1318
Preprint. Discussion started: 11 March 2021


Atmospheric Chemistry and Physics Discussions

1. Introduction

Stratiform clouds such as the stratus and stratocumulus clouds play an important role in global hydrologic and energy circulations (Warren et al. 1986, 1988; Stephens and Greenwald 1991; Hartmann et al. 1992; Hahn and Warren 2007; Wood, 2012). Aerosol concentrations have increased significantly as a result of industrialization. Increasing aerosols are known to decrease droplet size and thus increase the albedo of stratiform clouds (Twomey, 1974, 1977). Increasing aerosols may also suppress precipitation and, hence, alter the mass and lifetime of those clouds (Albrecht, 1989; Guo et al., 2016). These aerosol effects on stratiform clouds disrupt global hydrologic and energy circulations. However, these effects are highly uncertain and thus act to cause the highest uncertainty in the prediction of future climate (Ramaswamy et al., 2001; Forster et al., 2007). Most of the previous studies on stratiform clouds and their interactions with aerosols to reduce the uncertainty have dealt with warm stratiform clouds and have seldom considered ice-phase cloud particles (e.g., ice crystals) (Ramaswamy et al., 2001; Forster et al., 2007; Wood, 2012). In reality, especially during wintertime when the surface temperature approaches the freezing temperature, stratiform clouds frequently involve ice particles and associated processes such as deposition and freezing. Since particularly in midlatitudes, stratiform clouds are generally way below the level of homogeneous freezing, in these clouds, liquid and ice particles usually co-exist.

The level of water-vapor equilibrium saturation is lower for ice particles than for liquid particles. In mixed-phase clouds where liquid- and ice-phase hydrometeors coexist, this eventually induces ice (liquid) particles to experience supersaturation (undersaturation) for a certain amount of environmental water vapor. In this situation, liquid particles evaporate, while water vapor is deposited onto ice crystals. Water vapor in the air, which is depleted by the deposition onto ice crystals, is re-supplied by water vapor that is produced by the evaporation of droplets. The re-supplied water vapor in turn deposits onto ice crystals. In other words, due to differences in water-vapor equilibrium saturation between ice and liquid particles, ice particles eventually grow at the expense of liquid particles. This is so-called Wegener-Bergeron-Findeisen (WBF) mechanism (Wegener 1911; Bergeron 1935; Findeisen 1938). This mechanism changes the thermodynamic and dynamic environmental

https://doi.org/10.5194/acp-2020-1318
Preprint. Discussion started: 11 March 2021


Atmospheric Chemistry and Physics Discussions

conditions where cloud particles grow. Note that the development of clouds and its interactions with aerosols are strongly dependent on environmental thermodynamic and dynamic conditions such as humidity (saturation level), wind and stability (e.g., Khain et al., 2008; Lee et al., 2008). Hence, environmental conditions, affected by the WBF mechanism, are likely to result in the development of mixed-phase stratiform clouds and its interactions with aerosols that are different from those in warm clouds. However, the level of the understanding of the development of mixed-phase stratiform clouds and its interactions with aerosols has been very low.

Over the last decades, numerous studies have been performed to improve our understanding of mixed-phase clouds by focusing on clouds in the Arctic and over the Southern Ocean. It has been found that the prevalence of mixed-phase clouds over the Arctic enables them to have a substantial impact on radiative and hydrologic circulations (e.g., Shupe et al., 2001, 2005; Intrieri et al., 2002; Dong and Mace, 2003; Zuidema et al., 2005; Hu et al., 2010; Kanitz et al., 2011; Morrison et al., 2011; Huang et al., 2012). In addition, Rangno and Hobbs (2001), Lohmann (2002) and Borys et al. (2003) have proposed not only cloud condensation nuclei (CCN) but also ice nuclei (IN) affect mixed-phase clouds by altering microphysical variables (e.g., number concentrations and sizes of cloud particles) and dynamic variables (e.g., updrafts). However, Lance et al. (2010) and Jackson et al. (2012) have indicated that these aerosol effects on mixed-phase clouds have not been clearly identified due to lack of data of meteorological and cloud conditions in which aerosols influence those clouds. Naud et al. (2014) and Bodas-Salcedo et al. (2016) have reported that climate models have not been able to represent mixed-phased clouds and their interactions with aerosols reasonably well and this has been one important reason why climate models have produced large errors in simulating energy and hydrologic budgets and circulations.

This study aims to gain a better understanding of mixed-phase stratocumulus clouds and interactions between those clouds and aerosols. The better understanding enables us to gain a more general understanding of stratiform clouds and their interactions with aerosols, which better elucidates roles of clouds and aerosol-cloud interactions in climate. This in turn provides valuable information to better parameterize stratiform clouds and interactions for climate models. To fulfill the aim, this study focuses on effects of the interplay between

https://doi.org/10.5194/acp-2020-1318
Preprint. Discussion started: 11 March 2021


Atmospheric Chemistry and Physics Discussions

ice crystals and droplets on those clouds, and interactions of these effects with aerosols using a large-eddy simulation (LES) framework. The LES framework reasonably resolves microphysical and dynamic processes at turbulence scales and thus we can obtain process-level understanding of those effects and interactions.

Mixed-phase stratiform clouds have been formed frequently over the Korean Peninsula in midlatitudes and these clouds have been affected by the advection of aerosols from East Asia since its industrialization (e.g., Lee et al., 2013; Oh et al., 2015; Eun et al., 2016; Ha et al., 2019). However, we do not have a clear understanding of those clouds and impacts of those aerosols on them in the Peninsula (Eun et al., 2016). Motivated by this, we examine those clouds and effects of the advected aerosols from East Asia on them over an area in the Korean Peninsula as a way of better understanding those clouds and aerosol-cloud interactions in them.

2. Case description

A system of mixed-phase stratocumulus clouds was observed in the Seoul area in Korea over a period between 00 LST (local solar time) on January 12th and 00 LST on January 14th in 2013. The Seoul area is a conurbation area composed of the Seoul capital city and adjacent highly populated cities. The population of the Seoul area is estimated at twenty-five million. Coincidently, during this period, there is advection of an aerosol layer from the west of the Seoul area (or from East Asia) to it and this raises the level of aerosol concentrations in the Seoul area. This type of advection has been monitored by island stations in the Yellow Sea (Eun et al., 2016; Ha et al., 2019). For this study, the advection is monitored and identified by comparisons in PM_{10} and $PM_{2.5}$, representing aerosol mass, between a station in Baekryongdo island, located in the Yellow Sea, and stations in and around the Seoul area. PM stands for particulate matter and PM_{10} ($PM_{2.5}$) is the total mass of aerosol particles whose diameter is smaller than 10 (2.5) μm per unit volume of the air. In Figure 1, the island and the Seoul area are included in a rectangle that represents an area of interest in terms of the advection of the aerosol layer. Figure 2a shows the time series of PM_{10} and $PM_{2.5}$, measured by the station on the island and a representative station in the Seoul area, between January 10th and 19th in 2013 when there is strong advection of

https://doi.org/10.5194/acp-2020-1318
Preprint. Discussion started: 11 March 2021

Atmospheric Chemistry and Physics Discussions

aerosols from East Asia to the Seoul area. Around 00 LST on January 12th, aerosol mass starts to increase and reaches its peak at 10 LST on January 12th on the island. Then, there is a subsequent increase in aerosol mass in the Seoul area, which starts around 03 LST on January 12th, and it reaches its peak at 18 LST on January 12th in the Seoul area due to the advection of aerosols from East Asia to the Seoul area through the island. Figures 2b and 2c show observed aerosol mass distribution in the rectangle in Figure 1 at 03 LST and 18 LST on January 12th, respectively. Consistent with the time series, there is the high aerosol mass in and around the island due to the advection of aerosols from the East-Asia continent at 03 LST on January 12th (Figure 2b). Then, the advection continues to move aerosol mass eastward further to the Seoul area, resulting in a subsequent decrease in aerosol mass in and around the island and an increase in aerosol mass in the Seoul area at 18 LST on January 12th (Figure 2c). In this study, we examine how this advection of aerosols affects the observed mixed-phase stratocumulus clouds in the Seoul area.

3. LES and simulations

3.1 LES

As a LES model, we use the Advanced Research Weather Research and Forecasting (ARW) model (version 3.3.1), which is a nonhydrostatic compressible model (Michalakes et al., 2001; Klemp et al., 2007). Prognostic microphysical variables are transported with a 5th-order monotonic advection scheme (Wang et al., 2009). Shortwave and longwave radiation is parameterized by the Rapid Radiation Transfer Model (RRTM; Mlawer et al., 1997; Fouquart and Bonnel, 1980). The effective sizes of hydrometeors are calculated in an adopted microphysics scheme and the calculated sizes are transferred to the RRTM to consider effects of the effective sizes on radiation.

To represent microphysical processes, the LES model adopts a bin scheme based on the Hebrew University Cloud Model described by Khain et al. (2011). The bin scheme solves a system of kinetic equations for the size distribution functions of water drops, ice crystals or cloud ice (plate, columnar and branch types), snow aggregates, graupel and hail, as well as CCN and ice nuclei IN. Water drops whose size is smaller than 80 μm in diameter

https://doi.org/10.5194/acp-2020-1318
Preprint. Discussion started: 11 March 2021


Atmospheric Chemistry and Physics Discussions

are classified to be cloud droplets (or cloud liquid), while drops whose size is greater than 80 μm in diameter are classified to be rain drops (or rain). Each size distribution is represented by 33 mass doubling bins, i.e., the mass of a particle m_k in the kth bin is determined as $m_k = 2m_{k-1}$.

A cloud-droplet nucleation parameterization based on Köhler theory represents cloud-droplet nucleation. Arbitrary aerosol mixing states and aerosol size distributions can be fed to this parameterization. To represent heterogeneous ice-crystal nucleation, the parameterizations by Lohmann and Diehl (2006) and Möhler et al. (2006) are used. In these parameterizations, contact, immersion, condensation-freezing, and deposition nucleation paths are all considered by taking into account the size distribution of IN, temperature and supersaturation. Homogeneous aerosol (or haze particle) and droplet freezing is also considered following the theory developed by Koop et al. (2000).

3.2 Control run

For a three-dimensional simulation of the observed case of mixed-phase stratocumulus clouds, i.e., the control run, a domain with a 100-m resolution just over the Seoul area as shown in Figure 1 is adopted. The control run is for a period between 00 LST on January 12th and 00 LST on January 14th in 2013. The length of the domain in the east-west (north-south) direction is 220 (180) km. The 100 vertical layers with a terrain-following sigma coordinate are in the domain, and the model top is 500 hPa. This corresponds to the vertical resolution of 50 m on average.

Initial and boundary conditions of potential temperature, specific humidity, and wind for the simulation are provided by reanalysis data. These data are produced by the Met Office Unified Model (Brown et al., 2012) every 6 hours on a 0.11° × 0.11° grid. These data represent the synoptic-scale environment. An open lateral boundary condition is employed for the control run. Surface heat fluxes are predicted by the Noah land surface model (LSM; Chen and Dudhia, 2001).

The horizontally homogeneous aerosol properties are assumed in the current version of the ARW model. To consider the advection of aerosols and the associated spatiotemporal variation of aerosol properties such as composition and number

https://doi.org/10.5194/acp-2020-1318
Preprint. Discussion started: 11 March 2021


Atmospheric Chemistry and Physics Discussions

239 concentration, this assumption of the aerosol homogeneity is abandoned. For this
240 consideration, an aerosol preprocessor is developed to represent the variability of aerosol
241 properties. Observed background aerosol properties such as aerosol mass (e.g., PM_{10} and
242 $PM_{2.5}$) at observation sites are interpolated into model grid points and time steps by this
243 aerosol preprocessor.

244 Surface sites that measure $PM_{2.5}$ and PM_{10} in the domain observe the variability of
245 aerosol properties. Here, we assume that $PM_{2.5}$ and PM_{10} represent the mass of aerosols
246 that act as CCN. These sites resolve the variability with high spatiotemporal resolutions,
247 since they are distributed with about 1 km distance between them and measure aerosol
248 mass every ~10 minutes. However, they do not measure other aerosol properties such as
249 aerosol composition and size distributions. There are additional sites of the aerosol robotic
250 network (AERONET; Holben et al., 2001) in the domain with distances of ~10 km between
251 them. Hence, these AERONET sites provide data with coarser resolutions as compared to
252 those of the $PM_{2.5}$ and PM_{10} data, although information on aerosol composition and size
253 distributions are provided by the AERONET sites. In this study, the variability of properties
254 of aerosols that act as CCN over the domain is represented by using data from the high-
255 resolution $PM_{2.5}$/PM_{10} sites, while the relatively low-resolution data from the AERONET
256 sites are used to represent aerosol composition and size distributions.

257 According to AERONET measurements during the period with the observed
258 stratocumulus clouds, aerosol particles, on average, are an internal mixture of 70 %
259 ammonium sulfate and 30 % organic compound. This organic compound is assumed to be
260 water soluble and composed of (by mass) 18 % levoglucosan ($C_6H_{10}O_5$, density = 1600 kg
261 m^{-3}, van't Hoff factor = 1), 41 % succinic acid ($C_6O_4H_6$, density = 1572 kg m^{-3}, van't Hoff
262 factor = 3), and 41 % fulvic acid ($C_{33}H_{32}O_{19}$, density = 1500 kg m^{-3}, van't Hoff factor = 5)
263 based on a simplification of observed chemical composition. Aerosol chemical
264 composition in this study is assumed to be represented by this mixture. Aerosols before
265 their activation can affect radiation by changing the reflection, scattering, and absorption
266 of shortwave and longwave radiation. However, these impacts on radiation are not
267 considered in this study, since the mixture does not include a significant amount of
268 radiation absorbers such as black carbon. Based on the AERONET observation, as
269 exemplified in Figure 2d, the size distribution of background aerosols as CCN is assumed

https://doi.org/10.5194/acp-2020-1318
Preprint. Discussion started: 11 March 2021


Atmospheric Chemistry and Physics Discussions

to follow the tri-modal log-normal distribution. Stated differently, the size distribution of background aerosols as CCN in all parts of the domain during the whole simulation period is assumed to follow size distribution parameters or the shape of distribution as shown in Figure 2d. By averaging size distribution parameters (i.e., modal radius and standard deviation of each of nuclei, accumulation and coarse modes, and the partition of aerosol number among those modes) over the AERONET sites and the period with the stratocumulus clouds, the assumed shape of the size distribution of background aerosols is obtained. With the assumption above, $PM_{2.5}$ and PM_{10} are converted to the background number concentrations of aerosols as CCN.

For the control run, aerosol properties of IN and CCN are assumed to be identical except that the concentration of background aerosols as IN is assumed to be 100 times lower than the concentration of background aerosols as CCN at each of time steps and grid points. This is based on a general difference in concentration between CCN and IN (Pruppacher and Klett, 1978).

In clouds, aerosol sinks and sources control the evolution of aerosol size distribution. These sinks and sources include advection and aerosol activation (Fan et al., 2009). Activated particles are emptied in the corresponding bins of the aerosol spectra. Aerosol mass included in hydrometeors, after activation, is moved to different classes and sizes of hydrometeors through collision-coalescence and removed from the atmosphere once hydrometeors that contain aerosols reach the surface. Background aerosol concentrations are assumed not to vary with height in the planetary boundary layer (PBL), however, above the PBL, they are assumed to reduce exponentially with height. In non-cloudy areas, aerosol size and spatial distributions are set to follow background counterparts. In other words, once clouds disappear completely at any grid points, aerosol size distributions and number concentrations at those points recover to background counterparts. Numerous CSRM studies have adopted this method and proven that it is able to simulate overall aerosol properties and their impacts on clouds and precipitation reasonably well (Morrison and Grabowski, 2011; Lebo and Morrison, 2014; Lee et al., 2016). The impacts of cloud processes on the properties of background aerosols are not considered in this method. The above-described prescription of these properties (e.g., number concentration, size distribution, and chemical composition) means that aerosol physical and chemical

https://doi.org/10.5194/acp-2020-1318
Preprint. Discussion started: 11 March 2021


Atmospheric Chemistry and Physics Discussions

processes are not taken into account for this study. This enables us to isolate effects of given background aerosols on clouds in the domain by excluding those aerosol processes and cloud effects on background aerosol. Note that effects of background aerosols on clouds and precipitation in the domain as a part of the Korean Peninsula have not been well understood.

3.3 Additional runs

To examine effects of the aerosol advection on the observed stratocumulus clouds over the Seoul area, the control run is repeated by removing the increase in aerosol concentrations due to the aerosol advection. This repeated run is referred to as the low-aerosol run. In the low-aerosol run, to remove the increase in aerosol concentrations, background aerosol concentrations after 03 LST on January 12th do not evolve with the aerosol advection but is assumed to have background aerosol concentrations at 03 LST on January 12th at every time step and grid point only for the concentration of background aerosols acting as CCN. Here, the time- and domain-averaged concentration of background aerosols as CCN after 03 LST on January 12th in the low-aerosol run is lower than that in the control run by a factor of ~3. It is notable that there are no differences in the concentration of background aerosols acting as IN between the control and low-aerosol runs. This is to isolate effects of CCN, which accounts for most of aerosols, on clouds from those effects of IN via comparisons between the runs. Via the comparisons, we are able to identify how advection-induced increases in the concentration of aerosols acting as CCN affect clouds. The ratio of the concentration of background aerosols as CCN at 03 LST on January 12th to that after 03 LST on January 12th varies among grid points and time steps, since the concentration varies spatiotemporally throughout the simulation period in the control run. This means that a factor by which the concentration of background aerosols as CCN varies after 03 LST on January 12th between the control and low-aerosol runs is different for each of the time steps and grid points.

To examine effects of the interplay between ice crystals and droplets on the adopted system of stratocumulus clouds and its interactions with aerosols, the control and low-aerosol runs are repeated by removing ice processes. These repeated runs are referred to as

https://doi.org/10.5194/acp-2020-1318
Preprint. Discussion started: 11 March 2021


Atmospheric Chemistry and Physics Discussions

the control-noice and low-aerosol-noice runs. In the control-noice and low-aerosol-noice runs, only aerosols as CCN, droplets (i.e., cloud liquid), raindrops and associated microphysical processes (e.g., condensation and evaporation) exist, and aerosols as IN, all solid hydrometeors (i.e., ice crystals, snow, graupel, and hail) and associated processes (e.g., deposition and sublimation) are turned off, regardless of temperature. Via comparisons between the control and control-noice runs, we aim to identify effects of the interplay on the adopted system. Via comparisons between a pair of the control and low-aerosol runs and that of the control-noice and low-aerosol-noice runs, we aim to identify effects of the interplay on interactions between the system and aerosols. Henceforth, the pair of the control and low-aerosol runs is referred to as the ice runs, while the pair of the control-noice and low-aerosol-noice runs is referred to as the noice runs.

To better understand findings in Section 4.1.1, which explain how the interplay between ice crystals and droplets affects stratocumulus clouds, the control run is repeated by increasing the concentration of background aerosols acting as IN by a factor of 10 and 100 at each time step and grid point. These repeated runs are detailed in Section 4.1.2 and referred to as the IN-10 and IN-100 runs, respectively. Table 1 summarizes all of the simulations in this study.

4. Results

4.1 Effects of the interplay between ice crystals and droplets on clouds

4.1.1 The control and control-noice runs

Figure 3a shows the time series of the domain-averaged liquid-water path (LWP), ice-water path (IWP) and water path (WP), which is the sum of LWP and IWP, for the control run, and LWP for the control-noice run. Since in the control-noice run, there are no ice particles, LWP acts as WP in the run. WP is higher in the control-noice run than in the control run throughout the whole simulation period, although at the initial stage before 20:00 LST on January 12th, differences in WP between the runs are not as significant as those after 20:00 LST on January 12th (Figure 3a). The differences in WP between the runs are greatest

https://doi.org/10.5194/acp-2020-1318
Preprint. Discussion started: 11 March 2021


Atmospheric Chemistry and Physics Discussions

around 00:00 LST on January 13th when WP reaches its maximum value in each of the runs (Figure 3a). These differences decrease as time goes by after around 00:00 LST on January 13th (Figure 3a). The time- and domain-averaged WP over the period between 00 LST (local solar time) on January 12th and 00 LST on January 14th is 18 g m^{-3} and 55 g m^{-3} in the control and control-noice runs, respectively. Associated with this, the WP peak value reaches 83 g m^{-3} in the control run, while the value reaches 230 g m^{-3} in the control-noice run (Figure 3a). Over most of the simulation period, IWP is greater than LWP in the control run except for the period between ~22:00 LST on January 12th and ~01:00 LST on January 13th (Figure 3a). In the control run, the time- and domain-averaged IWP and LWP are 11 g m^{-3} and 7 g m^{-3}, respectively. Results here indicate that when solid and liquid particles coexist, cloud mass, represented by WP, reduces a lot as compared to that when liquid particles alone exist. To evaluate the control run, satellite and ground observations can be utilized. In the case of the Moderate Resolution Imaging Spectroradiometer, one of representative polar orbiting image sensors on board satellites, it passes the Seoul area only at 10:30 am and 1:30 pm every day, hence, the sensor is not able to provide reliable data that cover the whole simulation period. Multifunctional Transport Satellites (MTSAT), which are geostationary satellites and available in the East Asia, do not provide reliable data of LWP and IWP, although they provide comparatively reliable data of cloud fraction and cloud-top height throughout the whole simulation period (Faller, 2005). Ground observations provide data of cloud fraction and cloud-bottom height throughout the whole simulation period. Hence, the simulated cloud fraction, and cloud-bottom and -top heights are compared to those from the MTSAT and ground observations. The average cloud fraction over time steps when the domain-averaged WP is not zero is 0.92 and 0.86 in the control run and observations, respectively. The average cloud-bottom and -top heights over time steps and grid points with non-zero WP are 230 (250) m and 1.3 (1.5) km in the control run (observations), respectively. Hence, the percentage difference in each of cloud fraction, cloud-bottom and -top heights between the control run and observations is ~ 10% and thus the control run is considered performed reasonably well for these variables.

Condensation and deposition as phase-transition processes are the main sources of cloud mass in the control run. Since in the control-noice run, there are no ice particles, deposition is absent, and thus, condensation alone acts as the main source of cloud mass.

https://doi.org/10.5194/acp-2020-1318
Preprint. Discussion started: 11 March 2021


Atmospheric Chemistry and Physics Discussions

As seen in Figure 3b, condensation rates in the control-noice run are much higher than the sum of condensation and deposition rates in the control run. Associated with this, there is greater cloud mass in the control-noice run than in the control run, although deposition is absent in the control-noice run. However, at the initial stage before 20:00 LST on January 12th, differences between the sum in the control run and condensation rate in the control-noice run are not significant as compared to those after 20:00 LST on January 12th (Figure 3b). Hence, those differences become significant and increase as time progresses after the initial stage. Those differences are greatest around 00:00 LST on January 13th when the sum in the control run or condensation rate in the control-noice run reaches its maximum value. The differences decrease as time goes by after around 00:00 LST on January 13th. Condensation rate, deposition rate in the control run, and condensation rate in the control-noice run are similar to LWP, IWP in the control run, and LWP in the control-noice run, respectively, in terms of their temporal evolutions (Figures 3a and 3b). This similarity confirms that deposition and condensation are the main sources of IWP and LWP, respectively, and control cloud mass. Thus, understanding the evolutions of condensation and deposition is equivalent to understanding those of LWP and IWP, respectively. Hence, in the following, to understand evolutions of cloud mass and its differences between the control and control-noice runs, we analyze evolutions of condensation, deposition, and their differences between the runs.

The qualitative nature of differences in WP, which represents cloud mass, over the whole simulation period between the control and control-noice runs is initiated and established during the initial stage of cloud development before 20:00 LST on January 12th (Figures 3a and 3b). Hence, to understand mechanisms that initiate differences in WP between the control and control-noice runs, deposition, condensation and associated variables are analyzed for the initial stage. Note that synoptic or environmental conditions such as humidity and temperature are identical between the control and control-noice runs. These conditions act as initial and boundary conditions for the simulations and thus initial and boundary conditions are identical between the runs. Also, during the initial stage, feedbacks between dynamics (e.g., updrafts) and microphysics just start to form and thus are not fully established as compared to those feedbacks after the initial stage. This enables us to perform analyses of deposition and condensation during the initial stage by reasonably

https://doi.org/10.5194/acp-2020-1318
Preprint. Discussion started: 11 March 2021


Atmospheric Chemistry and Physics Discussions

425 excluding a large portion of complexity caused by those feedbacks. Hence, those analyses
426 during the initial stage can provide a clearer picture of either microphysical or dynamic
427 mechanisms that control differences in results between the runs.
428 During the initial stage before 20:00 LST on January 12th, evaporation rates, averaged
429 over the cloud layer, are higher in the control run than in the control-noice run due to the
430 WBF mechanism which facilitates evaporation of droplets and deposition onto ice crystals
431 (Figure 3c). As seen in Figure 3c, the cloud layer is between ~200 m and ~1.5 km in the
432 control run, while it is between ~200 m and ~2.5 km in the control-noice run. Associated
433 with more evaporation, droplets disappear more, leading to a situation where cloud droplet
434 number concentration (CDNC) starts to be lower in the control run during the initial stage
435 (Figure 3d). Then, during the initial stage, the reduction in CDNC leads to a reduction in
436 condensation in the control run as compared to that in the control-noice run (Figure 3b).
437 Fewer droplets mean that there is a less integrated droplet surface area where condensation
438 occurs and this induces less condensation in the control run. However, aided by the WBF
439 mechanism, deposition is facilitated at the initial stage, and this leads to greater deposition
440 than condensation in the control run at the initial stage (Figure 3b). This deposition is
441 inefficient and the subsequent increase in deposition is not sufficient, so, the sum of
442 condensation and deposition rates in the control run is slightly lower than condensation
443 rate in the control-noice run at the initial stage (Figure 3b); this contributes to slightly lower
444 WP in the control run than in the control-noice run during the initial stage (Figure 3a).
445 Hence, slightly greater latent heating, which is associated with condensation, in the control-
446 noice run than that, which is associated with the sum of deposition and condensation, in
447 the control run develops during the initial stage. This leads to stronger feedbacks between
448 updrafts and latent heating in the control run than in the control-noice run after the initial
449 stage, which in turn result in much stronger updrafts after the initial stage in the control-
450 noice run than in the control run. Due to these much stronger updrafts after the initial stage,
451 the time- and domain-averaged updrafts over the whole simulation period are also much
452 greater in the control-noice run than in the control run (Figure 4a). The much stronger
453 updrafts after the initial stage produce much larger WP in the control-noice run than in the
454 control run after the initial stage (Figure 3a).

https://doi.org/10.5194/acp-2020-1318
Preprint. Discussion started: 11 March 2021


Atmospheric Chemistry and Physics Discussions

455 The WBF mechanism indicates that the surplus water vapor produced by evaporation
456 acts as an additional source of deposition. If water vapor, including the surplus water vapor,
457 is efficiently deposited onto ice crystals, then the reduced cloud mass, due to the increased
458 evaporation and the subsequently reduced CDNC and condensation, can be efficiently
459 compensated by the additional gain of solid mass via deposition in the control run. This
460 would lead to much smaller differences in WP between the control and control-noice runs
461 than simulated. Here, we hypothesize that the inefficient deposition of water vapor is
462 related to much lower cloud ice number concentration (CINC) as compared to CDNC. As
463 seen in Figures 4b and 4c, CINC is ~ 2 orders of magnitude lower than CDNC. Hence,
464 while there is a comparatively large number of droplets that can potentially produce lots of
465 water vapor via evaporation, there is comparatively a small number of ice crystals and thus
466 a small integrated surface area of ice crystals where water vapor can be deposited in the
467 control run. It is hypothesized that this leads to a situation where water vapor, including
468 that from the evaporation of lots of droplets, is not able to find enough surface area of ice
469 crystals for efficient deposition, eventually leading to the inefficient deposition of the
470 surplus water vapor in the control run.
471
472 **a. LWP and IWP frequency distributions**
473
474 As seen in Figure 5a, the control-noice run has the lower (higher) WP cumulative frequency
475 for WP below (above) ~ 100 g m^{-2} than the control run at the last time step. This means
476 that the lower average WP in the control run is mainly due to a reduction in WP above
477 ~100 g m^{-2} in the control run. Through the WBF mechanism in the presence of ice particles,
478 liquid particles evaporate and condensation reduces. Hence, the LWP frequency reduces
479 substantially in the control run as compared to that in the control-noice run (Figure 5b).
480 With this reduction, LWP above ~ 800 g m^{-2} disappears and there is in general two to three
481 orders of magnitude lower LWP frequency for LWP below ~ 800 g m^{-2} in the control run
482 than in the control-noice run (Figure 5b).
483 As seen in Figure 5b, at the last time step, there is the presence of IWP frequency in
484 addition to the LWP frequency in the control run. Through the WBF mechanism, which
485 facilitates deposition, the IWP frequency is greater than the LWP frequency for IWP below

https://doi.org/10.5194/acp-2020-1318
Preprint. Discussion started: 11 March 2021


Atmospheric Chemistry and Physics Discussions

~ 200 g m^{-2} in the control run. Particularly for IWP below ~ 100 g m^{-2}, the IWP frequency in the control run is greater than the LWP frequency in the control-noice run. This enables the greater WP frequency in the control run than in the control-noice run for WP below ~ 100 g m^{-2} in spite of the lower LWP frequency below ~100 g m^{-2} in the control run (Figures 5a and 5b). However, the lower IWP frequency for IWP above ~ 100 g m^{-2} in the control run than the LWP frequency for LWP above ~ 100 g m^{-2} in the control-noice run contributes to the lower WP frequency for WP above ~ 100 g m^{-2} in the control run (Figures 5a and 5b). The lower WP frequency for WP above ~ 100 g m^{-2} in the control run is also contributed by the lower LWP frequency for LWP above ~ 100 g m^{-2} in the control run (Figures 5a and 5b).

4.1.2 The IN-10 and IN-100 runs

To test above-mentioned hypothesis about comparatively low CINC and associated inefficient deposition, the control run is compared with the IN-10 and IN-100 runs (Table 1). In particular, in the IN-100 run, the concentration of background aerosols as IN becomes that of background aerosols as CCN. This may be unrealistic. However, the main purpose of the repeated runs is to test the hypothesis and it is believed that the high concentrations of background aerosols as IN in the repeated runs are able to clearly isolate the role of the IN concentration and CINC in WP by making a stark contrast in the IN concentration and CINC between the control and repeated runs.

As seen in Figure 6a, CINC averaged over grid points and time steps with non-zero CINC increases by factors of ~5 (~60), when the concentration of background aerosols as IN increases by a factor of 10 (100) from the control run to the IN-10 (IN-100) run. With these increases in CINC, the average radius of ice crystals decreases by ~15% and 25% in the IN-10 and IN-100 runs, respectively. This induces increases in the integrated surface area of ice crystals and thus deposition in the IN-10 and IN-100 runs as compared to those in the control run (Figures 3b, 6b and 6c). These increases in deposition are more, because of greater increases in the integrated surface area in the IN-100 run than in the IN-10 run (Figures 6b and 6c). Of interest is that the increase in deposition accompanies a decrease in condensation in the IN-10 and the IN-100 runs as compared to that in the control run

https://doi.org/10.5194/acp-2020-1318
Preprint. Discussion started: 11 March 2021


Atmospheric Chemistry and Physics Discussions

(Figures 3b, 6b and 6c). This is because due to more deposition, more water vapor is transferred from air to ice crystals, which leaves less water vapor for condensation in the IN-10 run and IN-100 runs than in the control run. Greater deposition leaves less water vapor for condensation, leading to less condensation in the IN-100 run than in the IN-10 run.

Associated with increases in deposition and decreases in condensation, IWP increases and LWP decreases in both of the IN-10 and IN-100 runs as compared to those in the control run. Since there are greater increases in deposition and greater decreases in condensation, these increases in IWP and decreases in LWP are greater in the IN-100 run than in the IN-10 run. The increasing deposition and IWP contribute to increases in WP, while the decreasing condensation and LWP contribute to decreases in WP in the IN-10 and IN-100 runs (not shown). Figure 7a shows that there are increases in WP in the IN-10 and IN-100 runs as compared to WP in the control run and those increases are greater in the IN-100 run than in the IN-10 run. This means that the increases in deposition and IWP outweigh the decreases in condensation and LWP, respectively, in the IN-10 and IN-100 runs. This outweighing is greater and leads to greater increases in WP in the IN-100 run than in the IN-10 run (Figure 7a). As seen in Figure 7a, the enhanced average WP in the IN-100 run (the IN-50 run) reaches ~90% (~50%) of that in the control-noice run, while the average WP in the control run accounts for only ~20% of that in the control-noice run. Here, comparisons among the control, IN-10 and IN-100 runs confirm the hypothesis that ascribes much lower WP in the control run than in the control-noice run to the comparatively low CINC and associated inefficient deposition in the control run.

a. LWP and IWP frequency distributions

With the increasing concentration of aerosols as IN and CINC from the control run to the IN-10 run to the IN-100 run, there are substantial increases in the IWP cumulative frequency, while there are substantial decreases in the LWP cumulative frequency at the last time step (Figure 7b). These increases in the IWP frequency accompany increases in the IWP maximum value from ~200 g m^{-3} in the control run to ~1200 g m^{-3} in the IN-100 run through ~500 g m^{-3} in the IN-10 run (Figure 7b). These decreases in the LWP frequency

https://doi.org/10.5194/acp-2020-1318
Preprint. Discussion started: 11 March 2021


Atmospheric Chemistry and Physics Discussions

548 accompany decreases in the LWP maximum value from ~700 g m^{-3} in the control run to
549 ~100 g m^{-3} in the IN-100 run through ~300 g m^{-3} in the IN-10 run (Figure 7b). The increases
550 in the IWP frequency outweigh decreases in the LWP frequency between the IN-10 and
551 IN-100 runs (the IN-10 and control run), leading to the greater average WP in the IN-100
552 run than in the IN-10 run (in the IN-10 run than in the control run).
553
554 **4.2 Aerosol-cloud interactions**
555
556 **4.2.1 CCN**
557
558 With advection-induced increases in aerosol concentrations between the control and
559 low-aerosol runs, there are aerosol-induced increases and decreases in IWP and LWP,
560 respectively (Figure 8a). The increases in IWP are outweighed by the decreases in LWP,
561 leading to aerosol-induced decreases in the average WP between the ice runs. As seen in
562 Figure 8b, the WP frequency is greater particularly for WP < ~300 g m^{-2}, leading to the
563 higher average WP in the low-aerosol run than in the control run. As seen in Figure 8c,
564 particularly for WP below ~200 g m^{-2}, the IWP frequency increases, while the LWP
565 frequency decreases with increasing aerosols between the ice runs. The increase in the IWP
566 frequency is not able to outweigh the decrease in the LWP frequency, leading to aerosol-
567 induced decreases in the average WP between the ice runs. Results here are contrary to
568 the conventional wisdom that increasing concentrations of aerosols as CCN tend to
569 increase WP in stratiform clouds (Albrecht, 1989).
570 Between the noice runs, there is an increase in LWP (i.e., WP) with the increasing
571 concentration of aerosols as CCN (Figure 8a). The greater LWP frequency, concentrated
572 in the LWP range between ~100 and ~600 g m^{-2}, leads to the greater average LWP or WP
573 in the control-noice run than in the low-aerosol-noice run (Figures 8b and 8c).
574
575 a. Ice runs
576
577 1) Condensation and evaporation
578

https://doi.org/10.5194/acp-2020-1318
Preprint. Discussion started: 11 March 2021


Atmospheric Chemistry and Physics Discussions

The qualitative nature of aerosol-induced differences in deposition, IWP, condensation and LWP over the whole simulation period between the ice runs is initiated and established during the initial stage of cloud development before 20:00 LST on January 12th (Figure 8a). To understand mechanisms that control aerosol-induced differences in deposition and condensation as a way of understanding mechanisms that control those differences in IWP and LWP, the time series of deposition rate, condensation rate and associated variables in each of the ice runs and differences in these variables between the ice runs is obtained for the initial stage. Since this study focuses on these differences in the variables as a representation of aerosol effects on clouds, in the following, the description of the differences is given in more detail by involving both figures and text as compared to the description of the variables in each of the ice runs, involving text only for the sake of brevity.

i. CDNC and its relation to condensation and evaporation

Evaporation and condensation rates are higher in the control run than in the low-aerosol run throughout the initial stage and up to ~15:30 LST on January 12th, respectively (Figure 9a). Increases in evaporation tend to make more droplets disappear, while increases in aerosol activation and condensation counteract the disappearance. The average CDNC over grid points and time steps with non-zero CDNC is larger in the control run than in the low-aerosol run not only over the initial stage but also over the whole simulation period (Figures 9a and 10a). This means that on average, the evaporatively-driven increases in the disappearance of droplets is outweighed by the activation- and/or condensationally-enhanced counteraction particularly during the initial stage with increasing aerosol concentrations between the ice runs. As marked by a green-dashed box in Figure 9a, there are steady and rapid temporal increases in the CDNC differences between the ice runs over a period from 12:50 to 13:20 LST on January 12th. This is due to steady and rapid temporal increases in CDNC, which are larger in the control run than in the low-aerosol run, over the period (Figure 9a). More droplets or higher CDNC provides a larger integrated surface area of droplets where evaporation and condensation of droplets occur, and thus acts as more sources of evaporation and condensation. With steady and rapid temporal increases

https://doi.org/10.5194/acp-2020-1318
Preprint. Discussion started: 11 March 2021


Atmospheric Chemistry and Physics Discussions

610 in CDNC as a source of evaporation and condensation, temporal increases in both
611 evaporation, which are linked to the WBF mechanism, and condensation show a jump (or
612 a surge or a rapid increase) in them for the period between 12:50 and 13:20 LST on January
613 12th in each of the ice runs. This jump is higher associated with the larger temporal increase
614 in CDNC in the control run than in the low-aerosol run, which induces differences in each
615 of evaporation and condensation between the ice runs to jump, as marked by a red-dashed
616 box in Figure 9a, during the time period.
617 The jump in differences in condensation between the ice runs is not as high as that in
618 differences in evaporation between the ice runs (Figure 9a). This situation accompanies the
619 fact that in each of the ice runs, the jump in evaporation is higher than that in condensation.
620 This means that differences in the jump between evaporation and condensation are greater
621 in the control run than in the low-aerosol run. Hence, evaporatively-driven jump in the
622 disappearance of droplets outweighs condensationally-driven jump in counteraction in
623 each of the ice runs and this outweighing is greater in the control run than in the low-aerosol
624 run during the period with the jumps. Due to this, the increasing temporal trend of CDNC
625 turns to its decreasing trend in each of the ice runs and this decreasing trend is larger in the
626 control run than in the low-aerosol run. This in turn turns the increasing temporal trend of
627 the CDNC differences between the ice runs to their decreasing trend around 13:30 LST on
628 January 12th (Figure 9a).
629 The decreasing temporal trend of CDNC contributes to a decreasing temporal trend
630 of each evaporation and condensation, starting around 13:30 LST on January 12th, by
631 reducing the integrated surface area of droplets in each of the ice runs. This decreasing
632 trend of each evaporation and condensation is larger associated with the larger decreasing
633 trend of CDNC in the control run than in the low-aerosol run. This induces the increasing
634 temporal trend of differences in each evaporation and condensation between the ice runs
635 to change into their decreasing temporal trend around 13:30 LST on January 12th (Figure
636 9a). The decreasing trend of evaporation in each of the ice runs is smaller than that in
637 condensation. Associated with this, the decreasing trend of differences in evaporation
638 between the ice runs is smaller than that in condensation (Figure 9a). Stated differently, the
639 temporal reduction in evaporation in each of the ice runs and its differences between the

https://doi.org/10.5194/acp-2020-1318
Preprint. Discussion started: 11 March 2021


Atmospheric Chemistry and Physics Discussions

runs from 13:30 LST on January 12th onwards during the initial stage occurs to a less extent as compared to those in condensation.

ii. Evaporation and condensation efficiency

For a given humidity, the increase in the surface-to-volume ratio of droplets increases the evaporation (condensation) efficiency by increasing the integrated surface area of droplets per unit volume or mass of droplets. Here, evaporation (condensation) efficiency is defined to be the mass of droplets that are evaporated (condensed) per unit volume or mass of droplets. Aerosol-induced increases in the surface-to-volume ratio and thus evaporation and condensation efficiency are caused by aerosol-induced increases in CDNC and associated decreases in the droplet size. Increasing CDNC, in turn, increases competition among droplets for given water vapor needed for their condensational growth, leading to decreases in the droplet size. The average droplet radius over grid points and time steps with non-zero CDNC is 7.3, 9.8, 8.7, and 10.5 μm in the control, low-aerosol, control-noice and low-aerosol-noice runs, respectively. It is notable that the WBF-mechanism-induced evaporation per unit volume of droplets is also strongly proportional to the surface-to-volume ratio of droplets (Pruppacher and Klett, 1978). Hence, between the ice runs, enhanced evaporation efficiency by aerosol-induced increases in the surface-to-volume ratio accompanies aerosol-enhanced WBF-mechanism-associated efficiency of evaporation.

With the steady and rapid temporal increase in CDNC, there is a steady and rapid temporal enhancement of the surface-to-volume ratio of droplets and evaporation efficiency in each of the ice runs between 12:50 and 13:20 LST on January 12th. Remember that these increases in CDNC are larger in the control run than in the low-aerosol run. This induces the greater temporal enhancement of the ratio and evaporation efficiency in the control run than in the low-aerosol run. The temporal enhancement of the ratio and evaporation efficiency accompanies temporally enhancing WBF-mechanism-related efficiency of evaporation. This accompaniment boosts evaporation and enables the jump in temporal increases in evaporation to be greater than that in condensation in each of the ice runs. In association with the larger steady and rapid temporal increase in CDNC in the

https://doi.org/10.5194/acp-2020-1318
Preprint. Discussion started: 11 March 2021


Atmospheric Chemistry and Physics Discussions

control run than in the low-aerosol run, the temporally enhancing WBF-mechanism-related efficiency of evaporation and its boost on evaporation enhance with increasing aerosol concentrations. This, in turn, enables greater aerosol-induced increases in evaporation than in condensation or the greater jump in differences in evaporation between the ices runs than that in condensation over the period between 12:50 and 13:20 LST on January 12th (Figure 9a).

Even when both evaporation and condensation rates decrease with time in association with the decreasing temporal trend of CDNC and the surface-to-volume ratio of droplets over a period after 13:30 LST on January 12th during the initial stage in each of the ice runs, evaporation (condensation) rates are maintained higher throughout the initial stage (up to ~15:30 LST) in association with the higher CDNC and surface-to-volume ratio of droplets in the control run than in the low-aerosol run (Figure 9a). The presence of the WBF mechanism facilitates evaporation and this acts against the temporal decrease in evaporation with time over the period in each of the ice runs. This counteraction by the WBF mechanism reduces the temporal decrease in evaporation and enables evaporation to reduce temporally to a less extent as compared to condensation in each of the ice runs for the period. This accompanies the differences in the temporal reduction between evaporation and condensation that are larger in the control run than in the low-aerosol run. This, in turn, enables differences in evaporation between the ice runs to reduce to a less extent as compared to those in condensation over the period (Figure 9a). Due to this, differences (or aerosol-induced increases) in evaporation and associated aerosol-induced increases in evaporation-driven negative buoyancy between the ice runs are higher than those in condensation and condensation-driven positive buoyancy, respectively, for the period (Figure 9a). This induces the decreasing temporal trend of differences or aerosol-induced increases in updraft mass fluxes between the ice runs over the period (Figure 9a). The decreasing temporal trend of aerosol-induced increases in updraft mass fluxes eventually leads to lower updraft mass fluxes in the control run than in the low-aerosol run, as represented by negative differences in updraft mass fluxes between the ice runs from ~15:30 LST onwards during the initial stage (Figure 9a). Associated with this, condensation becomes smaller in the control run, as represented by negative differences in

https://doi.org/10.5194/acp-2020-1318
Preprint. Discussion started: 11 March 2021


Atmospheric Chemistry and Physics Discussions

condensation between the ice runs from ~15:30 LST onwards during the initial stage (Figure 9a).

The role of the WBF mechanism described in this section can be clearly seen by comparing the ice runs in this section to the noice runs, with no WBF mechanism, detailed in the following Section b.

2) Deposition and condensation

The difference in deposition between the ice runs is negligible and does not vary much with time up to ~15:30 LST on January 12th when the difference starts to show its significant increase (Figure 9a). With the start of the decreasing temporal trend of condensation around 13:30 LST on January 12th, more water vapor, not used by condensation, becomes available for deposition as compared to that before 13:30 LST on January 12th in each of the ice runs. Remember that this decreasing trend is greater in the control run than in the low-aerosol run. Hence, from 13:30 LST on January 12th onwards, more water vapor is available for deposition in the control run than in the low-aerosol run. This leads to the start of larger aerosol-induced increases in deposition between the ice runs around 13:30 LST on January 12th as compared to those increases before ~ 13:30 LST on January 12th (Figure 9a). The decrease in condensation in the control run continues and its differences between the runs grow even after the negative differences in condensation between the runs start to appear around 15:30 LST on January 12th. Hence, aerosol-induced increases in the amount of water vapor, which is not used by condensation and available for deposition, continue even after 15:30 LST on January 12th. This enables aerosol-induced increases in deposition between the ice runs to continue even after 15:30 LST on January 12th (Figure 9a). This is despite the evaporation-driven lower updraft mass fluxes in the control run than in the low-aerosol run from ~ 15:30 LST on January 12th onwards (Figure 9a). This indicates that after ~ 15:30 LST on January 12th, the microphysical process (e.g., the WBF mechanism) which tends to increase deposition with increasing aerosol concentrations outweighs dynamic processes (i.e., updraft mass fluxes) which tend to reduce deposition with increasing aerosol concentrations.

https://doi.org/10.5194/acp-2020-1318
Preprint. Discussion started: 11 March 2021


Atmospheric Chemistry and Physics Discussions

731 The increasing temporal trend of aerosol-induced increases in deposition is not able
732 to outweigh the increasing trend of aerosol-induced decreases in condensation between the
733 ice runs after ~ 15:30 LST on January 12th (Figure 9a). As discussed in Section 4.1, due to
734 very low CINC as compared to CDNC, there is an insufficient integrated surface area of
735 ice crystals for the deposition of available water vapor in the control run. Remember that
736 there is no change in the background concentration of aerosols as IN between the ice runs.
737 Hence, as seen in Figure 9a, there are negligible differences in CINC between the ice runs,
738 although in comparison to the CINC differences, CDNC increases significantly with
739 increasing aerosols between the ice runs. Hence, the ratio of CINC to CDNC is lower in
740 the control run than in the low-aerosol run. This indicates that CINC per unit CDNC and
741 associated unit evaporation is lower in the control run. Hence, the available water vapor,
742 including that from droplet evaporation, has more difficulty in finding the surface area of
743 ice crystals for deposition in the control run. Remember that there is more available water
744 vapor for deposition, which increases deposition more in the control run than in the low-
745 aerosol run, after ~ 13:30 LST on January 12th as compared to that before ~ 13:30 LST on
746 January 12th. However, the more difficulty in finding the surface area of ice crystals for
747 deposition makes the deposition of the more available water vapor less efficient in the
748 control run than in the low-aerosol run. This damps down the increase in deposition
749 particularly after ~ 13:30 LST on January 12th in the control run. Then, aerosol-induced
750 increases in deposition are not large enough to overcome aerosol-induced decreases in
751 condensation in the control run particularly after ~ 15:30 LST on January 12th (Figure 9a).
752 This in turn leads to the lower average WP in the control run than in the low-aerosol run
753 over the whole simulation period.
754
755 b. Noice runs
756
757 As between the ice runs, between the noice runs, the activation- and condensationally-
758 enhanced counteraction outweighs the evaporation-induced decreases in CDNC, leading
759 to increases in CDNC with increasing aerosol concentrations (Figures 9a, 9b, and 10b).
760 However, in the noice runs, ice processes, the associated WBF mechanism and increase in
761 the WBF-mechanism-associated efficiency of evaporation with increasing aerosol

https://doi.org/10.5194/acp-2020-1318
Preprint. Discussion started: 11 March 2021


Atmospheric Chemistry and Physics Discussions

762 concentrations are absent, although aerosol-induced increases in the surface-to-volume
763 ratio of droplets are present. The boost of evaporation by the WBF mechanism in each of
764 the ice runs leads to greater evaporation efficiency in the control run than in the control-
765 noice run and in the low-aerosol run than in the low-aerosol-noice run over the initial stage.
766 Aerosol-induced increases in the boost lead to aerosol-induced greater increases in
767 evaporation efficiency between the ice runs than between the noice runs over the initial
768 stage. Evaporation efficiency in the control, low-aerosol, control-noice, and low-aerosol-
769 noice runs is 1.61, 0.90, 0.21, and 0.12 %, respectively. Here, to obtain evaporation
770 efficiency, the cumulative values of evaporation and cloud-liquid mass at the last time step
771 of the initial stage are calculated as follows:
772
773 $$A\ cumulative\ value\ of\ an\ arbitrary\ variable\ "A" = \iint AdVdt \quad (1)$$
774
775 Here, $dV = dxdydz$ and t represents time. x, y and z represent displacement in east-west,
776 north-south and vertical directions, respectively. Evaporation rate in a unit volume of air,
777 which is in a unit of kg m^{-3} s^{-1}, at each grid point and time step is put into Eq. (1) as "A" to
778 obtain the cumulative value of evaporation. To obtain the cumulative value of cloud-liquid
779 mass, cloud-liquid mass in a unit volume of air at each grid point and time step is first
780 divided by the time step. This divided cloud-liquid mass, which is also in a unit of kg m^{-3}
781 s^{-1}, represents cloud-liquid mass per unit time and volume and is put into Eq. (1) as "A" to
782 obtain the cumulative value of cloud-liquid mass. Then, the cumulative evaporation is
783 divided by the cumulative cloud-liquid mass to obtain the evaporation efficiency for each
784 of the runs.
785 With temporal increases in CDNC, which are larger in the control-noice run than in
786 the low-aerosol-noice run, leading to those in CDNC differences between the noice runs,
787 there are temporal increases in condensation and evaporation, which are larger in the
788 control-noice run than in the low-aerosol-noice run, and thus in their differences between
789 the noice runs (Figure 9b). Associated with aerosol-induced smaller increases in
790 evaporation efficiency between the noice runs, aerosol-induced increases in condensation
791 are always greater than aerosol-induced increases in evaporation between the noice runs
792 during the initial stage (Figure 9b). This maintains aerosol-induced increases in updraft

https://doi.org/10.5194/acp-2020-1318
Preprint. Discussion started: 11 March 2021


Atmospheric Chemistry and Physics Discussions

mass fluxes between the noice runs and leads to aerosol-induced increases in WP between the noice runs. In contrast to this, in the ice runs, after ~12:50 LST on January 12th, aerosol-induced increases in condensation become lower than those in evaporation, leading to aerosol-induced lower updrafts and WP (Figure 9a). This comparison between the ice and noice runs confirms that the presence of ice processes and the associated WBF mechanism plays a critical role in smaller aerosol-induced increases in condensation than in evaporation in the ice runs. Figure 11 schematically depicts the flow of processes that are described in Section 4.2.1.

4.2.2 IN

So far, we have examined effects of the increasing concentration of aerosols acting as CCN. However, unlike situations in warm stratocumulus clouds that have garnered most of attention in terms of aerosol-cloud interactions, not only aerosols acting as CCN but also those acting as IN can affect mixed-phase stratocumulus clouds (Rangno and Hobbs, 2001; Lohmann, 2002; Borys et al., 2003). The above-described IN-10 and IN-100 runs as compared to the control run identifies how the increasing concentration of aerosols as IN affects mixed-phase clouds. As seen in this comparison, the increasing concentration of aerosols as IN causes WP to increase, contrary to effects of the increasing concentration of aerosols as CCN. However, at each time step and grid point, a factor by which the concentration of background aerosols as CCN varies between the control and low-aerosol runs is different from that by which the concentration of background aerosols as IN varies among the control, IN-10 and IN-100 runs. For better comparisons between CCN and IN effects, it is better to make consistency in the factors between simulations for CCN effects and those for IN effects. For this consistency, the control run is repeated by reducing the concentration of background aerosols acting as IN (but not CCN) at each time step and grid point by the same factor as used for the reduction in the concentration of background aerosols acting as CCN in the low-aerosol run as compared to that in the control run. This repeated run is referred to as the IN-reduced run and compared to the control run to examine the IN effects. The IN-reduced run is identical to the low-aerosol run except that the

https://doi.org/10.5194/acp-2020-1318
Preprint. Discussion started: 11 March 2021


Atmospheric Chemistry and Physics Discussions

823 concentration of background aerosols acting as IN but not CCN at every time step and grid
824 point after 03 LST on January 12th is assumed to have that at 03 LST on January 12th.
825 Figure 9c shows the time series of differences in deposition rate, condensation rate
826 and related variables between the control and IN-reduced runs. With the increasing
827 concentration of background aerosols as IN, there are more increases in CINC between
828 those runs than between the control and low-aerosol runs (Figures 9a and 9c). During the
829 initial stage before 20 LST on January 12th, overall, there is an increasing temporal trend
830 in differences in CINC between the control and IN-reduced runs due to the larger increasing
831 temporal trend in CINC in the control run than in the IN-reduced run (Figure 9c). Increasing
832 CINC provides the increasing integrated surface area of ice crystals for deposition. This
833 leads to the increasing temporal trend in deposition, which is larger in the control run, and
834 in differences in deposition between the control and IN-reduced runs (Figure 9c). However,
835 due to no changes in the concentration of the background aerosols as CCN between the
836 control and IN-reduced runs, there are negligible differences in CDNC between the control
837 and IN-reduced runs as compared to those between the control and low-aerosol runs
838 (Figures 9a and 9c). More deposition induces more evaporation via the WBF mechanism
839 in the control run than in the IN-reduced run (Figure 9c). Between the IN-reduced and
840 control runs, with no increases in the concentration of background aerosols as CCN,
841 increases in the surface-to-volume ratio and the associated enhancement in the WBF-
842 mechanism-related efficiency of evaporation are negligible as compared to those between
843 the control and low-aerosol runs. This contributes to aerosol-induced smaller increases in
844 evaporation between the control and IN-reduced runs than between the control and low-
845 aerosol runs (Figures 9a and 9c).
846 Mainly due to the increase in evaporation, there is more negative buoyancy and
847 updraft mass fluxes start to reduce in the control run as compared to those in the IN-reduced
848 run around 12:50 LST on January 12th (Figure 9c). Eventually, updraft mass fluxes in the
849 control run become smaller than those in the IN-reduced run around 15:50 LST on January
850 12th (Figure 9c). This decrease occurs to a lesser extent mainly due to smaller aerosol-
851 induced increases in evaporation between the control and IN-reduced runs than between
852 the control and low-aerosol runs (Figures 9a and 9c). Associated with weaker updrafts in
853 the control run, condensation in the control run becomes smaller than that in the IN-reduced

https://doi.org/10.5194/acp-2020-1318
Preprint. Discussion started: 11 March 2021


Atmospheric Chemistry and Physics Discussions

run around 15:50 LST on January 12th but to a lesser degree as compared to that between the control and low-aerosol runs (Figures 9a and 9c).

When there is aerosol-induced reduction in condensation, there starts to be more available water vapor for deposition and thus aerosol-induced increases in deposition between the control and IN-reduced runs jump around 15:50 LST on January 12th (Figure 9c). This is similar to the situation between the control and low-aerosol runs. However, due to greater aerosol-induced increases in CINC and the associated integrated surface area of ice crystals, after ~ 15:50 LST on January 12th, there are greater aerosol-induced increases in deposition between the control and IN-reduced runs than between the control and low-aerosol runs (Figures 9a and 9c). Remember that the decrease in condensation, starting around 15:50 LST on January 12th, between the control and IN-reduced runs is smaller than that between the control and low-aerosol runs. This enables the increase in deposition to overcome the decrease in condensation between the control and IN-reduced runs. The larger increase in deposition than the decrease in condensation between the control and IN-reduced runs eventually makes updrafts in the control run greater than those in the IN-reduced run around 18:50 LST on January 12th (Figure 9c).

Initiated by aerosol-induced greater increase in deposition during the initial stage, there is aerosol-induced greater increase in IWP between the control and IN-reduced runs than between the control and low-aerosol runs over the whole simulation period (Figure 12). Initiated by aerosol-induced smaller decrease in condensation during the initial stage, there is aerosol-induced smaller decrease in LWP between the control and IN-reduced runs than between the control and low-aerosol runs over the whole simulation period (Figure 12). This greater increase in IWP dominates over the smaller decrease in LWP between the control and IN-reduced runs, leading to an increase in WP in the control run as compared to that in the IN-reduced run. This is in contrast to the situation between the control and low-aerosol runs. Hence, comparisons between the control, IN-reduced and the low-aerosol runs demonstrate that whether there is an increasing concentration of aerosols as IN or CCN has substantial impacts on how WP responds to the increasing concentration of aerosols.

5. Summary and conclusions

https://doi.org/10.5194/acp-2020-1318
Preprint. Discussion started: 11 March 2021


Atmospheric Chemistry and Physics Discussions

When it comes to stratocumulus clouds and their interactions with aerosols, warm clouds, which are composed of liquid particles only, have garnered most of the attention. However, in mid-latitudes, particularly during the wintertime, there are frequent occurrences of mixed-phase stratocumulus clouds, which are composed of both liquid and solid particles. The level of understanding of mechanisms that control the development of these mixed-phase clouds and their interactions with aerosols has been low. Motivated by this, this study aims to improve our understanding of the development of these mixed-phase stratocumulus clouds and their interactions with aerosols by focusing on roles of ice particles and processes in the development and interactions.

Ice crystals (i.e., cloud ice) and their interactions with droplets (i.e., cloud liquid) via the WBF mechanism in a selected system of mixed-phase stratocumulus clouds lower cloud mass substantially as compared to that in warm stratocumulus clouds. Through the WBF mechanism between ice crystals (i.e., cloud ice) and droplets (i.e., cloud liquid) in the mixed-phase clouds, there are significant increases in the evaporation of droplets. This involves the disappearance of droplets, and subsequently increases in water vapor. These increases in water vapor enhance deposition. However, the increased water vapor or the surplus water vapor is not deposited onto ice crystals efficiently due to the much lower concentrations of aerosols as IN and CINC than the concentrations of aerosols as CCN and CDNC, respectively. This results in the much lower average cloud mass (i.e., WP) in the mixed-phase clouds than in the warm clouds. As the concentration of aerosols as IN and CINC increases, deposition enhances and this enables cloud mass in the mixed-phase clouds to be similar to that in the warm clouds.

In the mixed-phase clouds, with the increasing concentration of aerosols as CCN, there are decreases in cloud mass. In the mixed-phase clouds, aerosol-induced increases in the evaporation of droplets, which involve the WBF mechanism, and their impacts on updrafts outweigh aerosol-intensified feedbacks between condensation and updrafts. This leads to aerosol-induced decreases in cloud mass. However, in the warm clouds, with the increasing concentration of aerosols as CCN, there are increases in cloud mass. Due to the absence of the WBF mechanism, in the warm clouds, aerosol-induced increases in the evaporation of droplets are not as efficient as in the mixed-phase clouds. This enables aerosol-intensified

https://doi.org/10.5194/acp-2020-1318
Preprint. Discussion started: 11 March 2021


Atmospheric Chemistry and Physics Discussions

916 feedbacks between condensation and updrafts to induce aerosol-induced increases in cloud
917 mass in the warm clouds. With the increases in the concentration of aerosols as IN, there
918 are aerosol-induced greater increases in CINC and deposition than with the increases in the
919 concentration of aerosols as CCN. This enables the increasing concentration of aerosols as
920 IN to induce increases in cloud mass, which is in contrast to the situation with the
921 increasing concentration of aerosols as CCN. The increasing concentration of aerosols as
922 CCN does not increase CINC and thus deposition as significantly as the increasing
923 concentration of aerosols as IN, leading to a situation where increases in evaporation
924 dominate the response of cloud mass to the increasing concentration of aerosols.
925 It is generally true that the conventional wisdom of stratiform clouds and aerosol
926 effects on them has been established mostly by relying on warm clouds (Ramaswamy et
927 al., 2001; Forster et al., 2007; Wood, 2012). For example, this wisdom generally indicates
928 that increasing concentrations of aerosols as CCN increase cloud mass (Albrecht, 1989).
929 However, in contrast to this, this study shows that in the mixed-phase stratiform clouds,
930 the increasing concentration of aerosols as CCN can reduce cloud mass through the WBF
931 mechanism which involves efficient evaporation of droplets and inefficient deposition of
932 water vapor onto ice crystals. It is also shown that the increasing concentration of aerosols
933 as IN enhances cloud mass in contrast to roles of the increasing concentration of aerosols
934 as CCN in cloud mass. In addition, this study finds that the WBF mechanism reduces cloud
935 mass in the mixed-phase clouds as compared to that in warm clouds. Mid-latitude winter
936 stratiform clouds and high-latitude clouds such as the Arctic stratiform clouds frequently
937 involve ice particles as well as liquid particles and hence are affected by the WBF
938 mechanism and IN. As discussed in Stevens and Feingold (2009), our lack of understanding
939 of these clouds and their interactions with aerosols has made a significant contribution to
940 the high uncertainty in the prediction of climate change. Hence, to reduce this uncertainty
941 especially by reducing the related uncertainty in climate models, we have to go beyond the
942 warm-cloud-based traditional parameterizations of clouds and their interactions with
943 aerosols in climate models. For this, this study indicates that it is imperative to develop
944 new parameterizations that consider the impacts of the WBF mechanism and IN on clouds
945 and their interactions with aerosols.
946

https://doi.org/10.5194/acp-2020-1318
Preprint. Discussion started: 11 March 2021

Atmospheric Chemistry and Physics Discussions

947 **Code/Data availability**

948 The Code/data used are currently private and stored in our private computer system.
949 Opening the data to the public requires approval from funding sources. Since funding
950 projects associated with this work are still going on, these sources do not allow the data to
951 be open to the public; 2–3 years after these project ends, the data can be open to the public.
952 However, if there is any inquiry about the data, contact the corresponding author Seoung
953 Soo Lee (slee1247@umd.edu).

954

955 **Author contributions**

956 SSL and KJH established essential initiative ideas to start this work. While SSL worked on
957 the analysis of simulation data, KJH and MGM worked on the analysis of observation data.
958 MK, HK, NU, and JG participated in the preliminary analysis of simulation and
959 observation data, and provided ideas to improve the presentation of results by reviewing
960 the manuscript.

961

962 **Competing interests**

963 The authors declare that they have no conflict of interest.

964
965
966
967
968
969
970
971
972
973
974
975
976
977
978
979
980
981
982
983
984
985

https://doi.org/10.5194/acp-2020-1318
Preprint. Discussion started: 11 March 2021

Atmospheric Chemistry and Physics Discussions

Acknowledgements

This study is supported by the National Research Foundation of Korea (NRF) grant funded by the Korea government (MSIT) (No. NRF2020R1A2C1003215) and the "Construction of Ocean Research Stations and their Application Studies" project, funded by the Ministry of Oceans and Fisheries, South Korea

https://doi.org/10.5194/acp-2020-1318
Preprint. Discussion started: 11 March 2021

Atmospheric Chemistry and Physics Discussions

References

Albrecht, B. A.: Aerosols, cloud microphysics, and fractional cloudiness, Science, 245, 1227-1230, 1989.

Bergeron, T.: On the physics of clouds and precipitation. Proces Verbaux de l'Association de Meteorologie, International Union of Geodesy and Geophysics, 156–178, 1935.

Bodas-Salcedo, A., Hill, P. G., Furtado, K., Williams, K. D., Field, P. R., Manners, J. C., Hyder, P. and Kato, S.: Large contribution of supercooled liquid clouds to the solar radiation budget of the Southern Ocean, J. Climate, 29, 4213–4228, doi:10.1175/JCLI-D-15-0564.1, 2016.

Borys, R. D., Lowenthal, D. H., Cohn, S. A. and Brown, W. O. J.: Mountaintop and radar measurements of anthropogenic aerosol effects on snow growth and snowfall rate. Geophys. Res. Lett., 30, 1538, doi:10.1029/2002GL016855 ,2003.

Brown, A., Milton, S., Cullen, M., Golding, B., Mitchell, J., and Shelly, A.: Unified modeling and prediction of weather and climate: A 25-year journey, Bull. Am Meteorol. Soc. 93, 1865–1877, 2012.

Chen, F., and Dudhia, J.: Coupling an advanced land-surface hydrology model with the Penn State-NCAR MM5 modeling system. Part I: Model description and implementation, Mon. Wea. Rev., 129, 569–585, 2001.

Dong, X., and Mace, G. G.: Arctic stratus cloud properties and radiative forcing derived from ground-based data collected at Barrow, Alaska. J. Climate, 16, 445–461, doi:10.1175/1520-0442(2003)016,0445:ASCPAR.2.0.CO;2, 2003.

Eun, S.-H., Kim, B.-G., Lee, K.-M., and Park, J.-S.: Characteristics of recent severe haze events in Korea and possible inadvertent weather modification, SOLA, 12, 32-36, 2016.

Faller, K: MTSAT-1R: A multifunctional satellite for Japan and the Asia-Pacific region, Proceedings of the 56th IAC 2005, Fukuoda, Japan, Oct. 17-21, 2005, IAC-05-B3.2.04

Fan, J., Yuan, T., Comstock, J. M., et al.: Dominant role by vertical wind shear in regulating aerosol effects on deep convective clouds, J. Geophys. Res., 114, doi:10.1029/2009JD012352, 2009.

https://doi.org/10.5194/acp-2020-1318
Preprint. Discussion started: 11 March 2021

Atmospheric Chemistry and Physics Discussions

1048 Findeisen, W.: Kolloid-meteorologische Vorgange bei Neiderschlagsbildung. Meteor. Z.,
1049 55, 121–133, 1938.
1050 Forster, P., et al., Changes in atmospheric constituents and in radiative forcing, in: Climate
1051 change 2007: the physical science basis, Contribution of working group I to the Fourth
1052 Assessment Report of the Intergovernmental Panel on Climate Change, edited by
1053 Solomon, S., et al., Cambridge Univ. Press, New York, 2007.
1054 Fouquart, Y., and Bonnel, B.: Computation of solar heating of the Earth's atmosphere: a
1055 new parameterization, Beitr. Phys. Atmos., 53, 35-62, 1980.
1056 Guo, J., M. Deng, S. S. Lee, F. Wang, Z. Li, P. Zhai, H. Liu, W. Lv, W. Yao, and X. Li:
1057 Delaying precipitation and lightning by air pollution over the Pearl River Delta. Part
1058 I: Observational analyses, J. Geophys. Res. Atmos., 121, 6472–6488,
1059 doi:10.1002/2015JD023257, 2016.
1060 Ha, K.-J., Nam, S., Jeong, J.-Y., et al., Observations utilizing Korean ocean research
1061 stations and their applications for process studies, Bull. Amer. Meteor. Soc., 100,
1062 2061-2075, 2019.
1063 Hahn, C. J., and Warren, S. G.: A gridded climatology of clouds over land (1971–96) and
1064 ocean (1954–97) from surface observations worldwide. Numeric Data Package NDP-
1065 026EORNL/CDIAC-153, CDIAC, Department of Energy, Oak Ridge, TN, 2007.
1066 Hartmann, D. L., Ockert-Bell, M. E., and Michelsen, M. L.: The effect of cloud type on
1067 earth's energy balance—Global analysis, J. Climate, 5, 1281–1304, 1992.
1068 Holben, B. N., Tanré, D., Smirnov, et al.: An emerging ground-based aerosol climatology:
1069 Aerosol optical depth from AERONET, J. Geophys. Res., 106, 12067–12097, 2001.
1070 Hu, Y., Rodier, S., Xu, K.-M., Sun, W., Huang, J., Lin, B., Zhai, P., and Josset, D.:
1071 Occurrence, liquid water content and fraction of supercooled water clouds from
1072 combined CALIOP/IIR/MODIS measurements, J. Geophys. Res., 115, D00H34,
1073 doi:10.1029/2009JD012384, 2010.
1074 Huang, Y., Siems, S. T., Manton, M. J., Protat, A. and Delanöe, J.: A study on the low-
1075 altitude clouds over the Southern Ocean using the DARDAR-MASK, J. Geophys.
1076 Res., 117, D18204, doi:10.1029/2012JB009424, 2012.
1077 Intrieri, J. M., Shupe, M. D., Uttal, T. and McCarty, B. J.: An annual cycle of Arctic cloud
1078 characteristics observed by radar and lidar at SHEBA, J. Geophys. Res., 107, 8030,

https://doi.org/10.5194/acp-2020-1318
Preprint. Discussion started: 11 March 2021

Atmospheric Chemistry and Physics Discussions

1079 doi:10.1029/2000jc000423, 2002.
1080 Jackson, R. C., and Coauthors: The dependence of Arctic mixed-phase stratus ice cloud
1081 microphysics on aerosol concentration using observations acquired during ISDAC
1082 and M-PACE, J. Geophys. Res., 117, D15207, doi:10.1029/2012JD017668, 2012.
1083 Kanitz, T., Seifert, P., Ansmann, A., Engelmann, R., Althausen, D., Casiccia, C. and
1084 Rohwer, E. G.: Contrasting the impact of aerosols at northern and southern
1085 midlatitudes on heterogeneous ice formation, Geophys. Res. Lett., 38,
1086 L17802,doi:10.1029/2011GL048532, 2011.
1087 Khain, A., BenMoshe, N. and Pokrovsky, A.: Factors determining the impact of aerosols
1088 on surface precipitation from clouds: Attempt of classification, J. Atmos. Sci., 65,
1089 1721 – 1748, 2008.
1090 Khain, A., Pokrovsky, A., Rosenfeld, D., Blahak, U., and Ryzhkoy, A.: The role of CCN in
1091 precipitation and hail in a mid-latitude storm as seen in simulations using a spectral
1092 (bin) microphysics model in a 2D dynamic frame, Atmos. Res., 99, 129–146, 2011.
1093 Klemp, J. B., Skamarock, W. C., and Dudhia, J.: Conservative split-explicit time
1094 integration methods for the compressible nonhydrostatic equations, Mon. Weather
1095 Rev., 135, 2897 – 2913, 2007.
1096 Koop, T., Luo, B. P., Tsias, A. and Peter, T.: Water activity as the determinant for
1097 homogeneous ice nucleation in aqueous solutions, Nature, 406, 611-614, 2000.
1098 Lance, S., Brock, C. A., Rogers, D. and Gordon, J. A.: Water droplet calibration of the
1099 Cloud Droplet Probe (CDP) and inflight performance in liquid, ice and mixed-phase
1100 clouds during ARCPAC, Atmos. Meas. Tech., 3, 1683–1706, doi:10.5194/amt-3-
1101 1683-2010, 2010.
1102 Lebo, Z. J., and Morrison, H.: Dynamical effects of aerosol perturbations on simulated
1103 idealized squall lines, Mon. Wea. Rev., 142, 991-1009, 2014.
1104 Lee, S., Ho, C.-H., Lee, Y. G., Choi, H.-J. and Song, C.-K.: Influence of transboundary air
1105 pollutants from China on the high-PM10 episode in Seoul, Korea for the period
1106 October 16−20, 2008. Atmos. Environ., 77, 430−439, 2013.
1107 Lee, S. S., Kim, B.-G., and Yum, S. S., et al.: Effect of aerosol on evaporation, freezing and
1108 precipitation in a multiple cloud system, Clim. Dyn., 48, 1069-1087, 2016.
1109 Lee, S. S., Donner, L. J., Phillips, V. T. J. and Ming, Y.: The dependence of aerosol effects

https://doi.org/10.5194/acp-2020-1318
Preprint. Discussion started: 11 March 2021

Atmospheric Chemistry and Physics Discussions

on clouds and precipitation on cloud-system organization, shear and stability. J. Geophys. Res., 113, D16202, doi:10.1029/2007JD009224, 2008.

Lohmann, U.:Aglaciation indirect aerosol effect caused by soot aerosols, Geophys. Res. Lett., 29, doi:10.1029/2001GL014357, 2002.

Michalakes, J., Chen, S., Dudhia, J., Hart, L., Klemp, J., Middlecoff, J. and Skamarock, W.: Development of a next generation regional weather research and forecast model, in Developments in Teracomputing: Proceedings of the Ninth ECMWF Workshop on the Use of High Performance Computing in Meteorology, edited by W. Zwieflhofer and N. Kreitz, pp. 269 – 276, World Sci., Singapore, 2001.

Mlawer, E. J., Taubman, S. J., Brown, P. D., Iacono, M. J., and Clough, S. A.: RRTM, a validated correlated-k model for the longwave, J. Geophys. Res., 102, 16663-1668, 1997.

Morrison, A. E., Siems, S. T. and Manton, M. J.: A three year climatology of cloud-top phase over the Southern Ocean and North Pacific, J. Climate, 24, 2405–2418,doi:10.1175/2010JCLI3842.1, 2011.

Morrison, H., and Grabowski, W. W.: Cloud-system resolving model simulations of aerosol indirect effects on tropical deep convection and its thermodynamic environment, Atmos. Chem. Phys., 11, 10503–10523, 2011.

Möhler, O., et al, Efficiency of the deposition mode ice nucleation on mineral dust particles, Atmos. Chem. Phys., 6, 3007-3021, 2006.

Naud, C., Booth, J. F. and Del Genio, A. D.: Evaluation of ERA-Interim andMERRA cloudiness in the Southern Ocean, J. Climate, 27, 2109–2124, doi:10.1175/JCLI-D-13-00432.1, 2014.

Oh, H.-R., Ho, C.-H., Kim, J., Chen, D., Lee, S., Choi, Y.-S., Chang, L.-S., and Song, C.-K.: Long-range transport of air pollutants originating in China: A possible major cause of multi-day high-PM10 episodes during cold season in Seoul, Korea. Atmos. Environ., 109, 23−30, 2015.

Pruppacher, H. R. and Klett, J. D.: Microphysics of clouds and precipitation, 714pp, D. Reidel, 1978.

Rangno, A. L., and Hobbs, P. V.: Ice particles in stratiform clouds in the Arctic and possible mechanisms for the production of high ice concentrations, J. Geophys. Res., 106,15

https://doi.org/10.5194/acp-2020-1318
Preprint. Discussion started: 11 March 2021

065–15 075, doi:10.1029/2000JD900286, 2001.

Ramaswamy, V., et al.: Radiative forcing of climate change, in Climate Change 2001: The Scientific Basis, edited by J. T. Houghton et al., 349-416, Cambridge Univ. Press, New York, 2001.

Shupe, M. D., Uttal, T., Matrosov, S, Y. and Rrisch, A. S.: Cloud water contents and hydrometeor sizes during the FIRE Arctic clouds experiment, J. Geophys. Res., 106, 15 015–15 028, doi:10.1029/2000JD900476, 2001.

Shupe, M. D., Uttal, T. and Matrosov, S. Y.: Arctic cloud microphysics retrievals from surface-based remote sensors at SHEBA, J. Appl. Meteor., 44, 1544–1562, doi:10.1175/JAM2297.1, 2005.

Stephens, G. L., and Greenwald, T. J.: Observations of the Earth's radiation budget in relation to atmospheric hydrology. Part II: Cloud effects and cloud feedback. J. Geophys. Res., 96, 15 325–15 340, 1991.

Stevens, B., and Feingold, G.: Untangling aerosol effects on clouds and precipitation in a buffered system, Nature, 461, 607-613, 2009.

Twomey, S.: The influence of pollution on the shortwave albedo of clouds, J. Atmos. Sci., 34, 1149-1152, 1977.

Twomey, S.: Pollution and the Planetary Albedo, Atmos. Env., 8,1251-1256, 1974.

Wang, H., Skamarock, W. C., and Feingold, G.: Evaluation of scalar advection schemes in the Advanced Research WRF model using large-eddy simulations of aerosol-cloud interactions, Mon. Wea. Rev., 137, 2547-2558, 2009.

Warren, S. G., Hahn, C. J., London, J., Chervin, R. M., and Jenne, R. L.: Global distribution of total cloud cover and cloud types over land. NCAR Tech. Note NCAR/TN-273+STR, National Center for Atmospheric Research, Boulder, CO, 29 pp. + 200 maps, 1986.

Wegener, A.: Thermodynamik der Atmosphare. J. A. Barth, 311 pp, 1911.

Wood, R.: Stratocumulus clouds, Mon. Wea. Rev., 140, 2373-2423, 2012.

Zuidema, P., Westwater, E. R., Fairall, C. and Hazen, D.: Ship-based liquid water path estimates in marine stratocumulus, J. Geophys. Res., 110, D20206, doi:10.1029/2005JD005833, 2005.

https://doi.org/10.5194/acp-2020-1318
Preprint. Discussion started: 11 March 2021


Atmospheric Chemistry and Physics Discussions

FIGURE CAPTIONS

Figure 1. A rectangle represents the domain of interest in terms of the aerosol advection. A dot in the rectangle marks Baekryongdo island and an area to the east of the yellow line in the rectangle is the Seoul area. In the Seoul area, a closed dotted line marks the boundary of the Seoul city.

Figure 2. (a) Time series of PM_{10} and $PM_{2.5}$ observed at the station in Baekryongdo island (BN) and a representative station in the Seoul area (SL). The abscissa represents dates between January 10th and 19th in 2013. The spatial distribution of $PM_{2.5}$ over the rectangle in Figure 1 at (b) 03 LST and (c) 18 LST on January 12th in 2013. (d) Aerosol size distribution at the surface. N represents aerosol number concentration per unit volume of air and D represents aerosol diameter.

Figure 3. Time series of (a) the domain-averaged liquid-water path (LWP), ice-water path (IWP) and water path (WP), which is the sum of LWP and IWP, for the control run, and LWP for the control-noice run, and (b) the domain-averaged condensation rates, deposition rates and the sum of those rates in the control run and condensation rates in the control-noice run. (c) Vertical distribution of the domain-averaged evaporation rates and (d) CDNC over grid points and time steps with non-zero CDNC for the initial stage between 00:00 LST and 20:00 LST on January 12th.

Figure 4. Vertical distributions of (a) the time- and domain-averaged updraft mass fluxes for the control and control-noice runs, (b) the average cloud droplet number concentration (CDNC) over grid points and time steps with non-zero CDNC and (c) cloud ice number concentration (CINC) over grid points and time steps with non-zero CINC for the whole domain and the simulation period in the control run.

Figure 5. Cumulative frequency of (a) WP in the control run and LWP, which is WP, in the control-noice run and (b) LWP and IWP in the control run and LWP in the control-noice run at the last time step.

https://doi.org/10.5194/acp-2020-1318
Preprint. Discussion started: 11 March 2021


Atmospheric Chemistry and Physics Discussions

Figure 6. (a) Vertical distributions of CINC over grid points and time steps with non-zero CINC for the whole domain and simulation period in the control, IN-10, and IN-100 runs. Time series of the domain-averaged condensation rates, deposition rates and the sum of those rates (b) in the IN-10 run and (c) in the IN-100 run. In (b) and (c), condensation rates in the control-noice run are additionally displayed.

Figure 7. (a) Time series of the domain-averaged LWP, IWP and WP for the control run, LWP for the control-noice run and WP for the IN-10 and IN-100 runs. (b) Cumulative frequency of LWP, IWP and WP for the control, IN-10 and IN-100 runs at the last time step.

Figure 8. (a) Time series of the domain-averaged LWP, IWP and WP for the control and low-aerosol runs, and LWP, which is also WP, for the control-noice and low-aerosol-noice runs. (b) Cumulative frequency of WP for the control, low-aerosol run, control-noice and low-aerosol-noice runs, and (c) LWP and IWP for the control and low-aerosol runs and LWP in the control-noice and low-aerosol-noice runs at the last time step.

Figure 9. Time series of differences in the domain-averaged updraft mass fluxes, deposition, condensation and evaporation rates, the average CDNC (CINC) over grid points with non-zero CDNC (CINC) (a) between the control and low-aerosol runs (the control run minus the low-aerosol run), (b) between the control-noice and low-aerosol-noice runs (the control-noice run minus the low-aerosol-noice run) and (c) between the control and IN-reduced runs (the control run minus the IN-reduced run). Dashed lines in (a), (b) and (c) represent zero differences. In (b), due to the absence of ice processes in the noice runs, differences in deposition rates and CINC are absent. A green-dashed box in (a) marks a time period when steady and rapid temporal increases in the CDNC differences between the ice runs occur, while a red-dashed box in (a) marks a time period when a jump in differences in evaporation rates between the control and low-aerosol runs occurs (see text for details).

https://doi.org/10.5194/acp-2020-1318
Preprint. Discussion started: 11 March 2021


Atmospheric Chemistry and Physics Discussions

Figure 10. (a) Vertical distributions of CDNC over grid points and time steps with non-zero CDNC for the whole domain and simulation period (a) in the control and low-aerosol runs, and (b) in the control-noice and low-aerosol-noice runs.

Figure 11. A schematic diagram that depicts the flow of processes that are described in Section 4.2.1 and associated with responses of clouds to increasing aerosols as CCN.

Figure 12. Time series of the domain-averaged LWP, IWP and WP for the control, low-aerosol and IN-reduced runs, and LWP, which is also WP, for the control-noice and low-aerosol-noice runs.

https://doi.org/10.5194/acp-2020-1318
Preprint. Discussion started: 11 March 2021

Atmospheric Chemistry and Physics Discussions

Simulations	Increases in the background concentration of aerosols as CCN due to the aerosol advection after 03 LST on January 12th	Ice processes	Background concentration of aerosols as IN
Control run	Present	Present	100 times lower than the background concentration of aerosols as CCN
Low-aerosol run	Absent	Present	Same as in the control run
Control-noice run	Present	Absent	Absent
Low-aerosol-noice run	Absent	Absent	Absent
IN-10 run	Present	Present	10 times higher than in the control run
IN-100 run	Present	Present	100 times higher than in the control run

Table 1. Summary of simulations

https://doi.org/10.5194/acp-2020-1318
Preprint. Discussion started: 11 March 2021

Atmospheric Chemistry and Physics Discussions

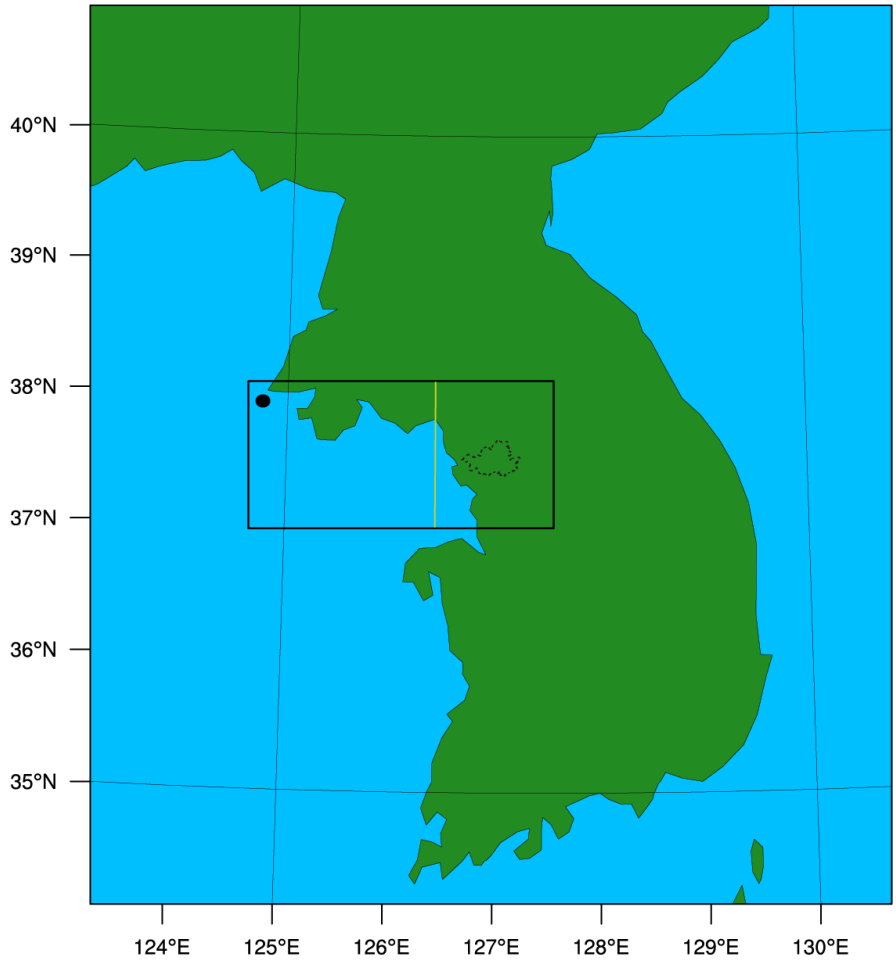

1275

1276 **Figure 1**

1277

1278

1279

1280

1281

https://doi.org/10.5194/acp-2020-1318
Preprint. Discussion started: 11 March 2021

Atmospheric Chemistry and Physics Discussions

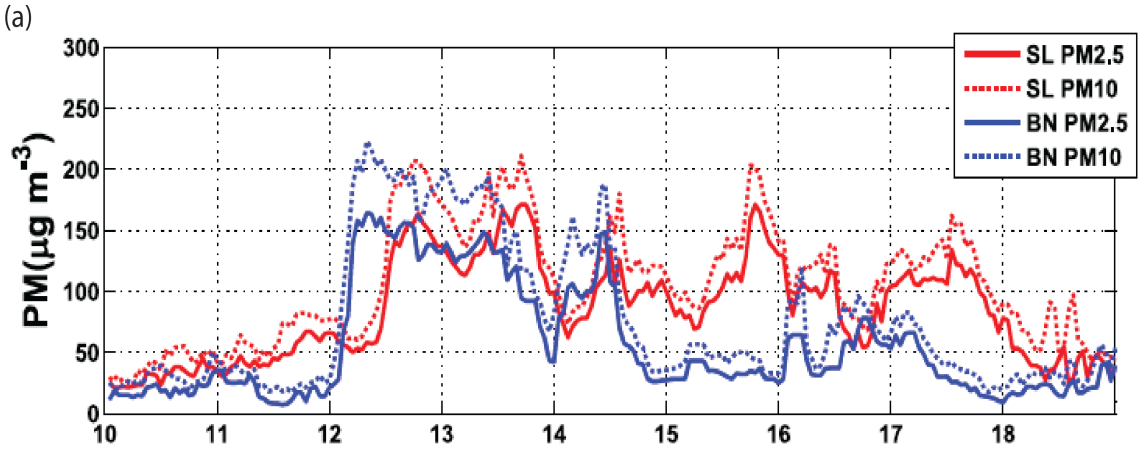

Figure 2a

https://doi.org/10.5194/acp-2020-1318
Preprint. Discussion started: 11 March 2021

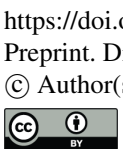

Atmospheric Chemistry and Physics Discussions

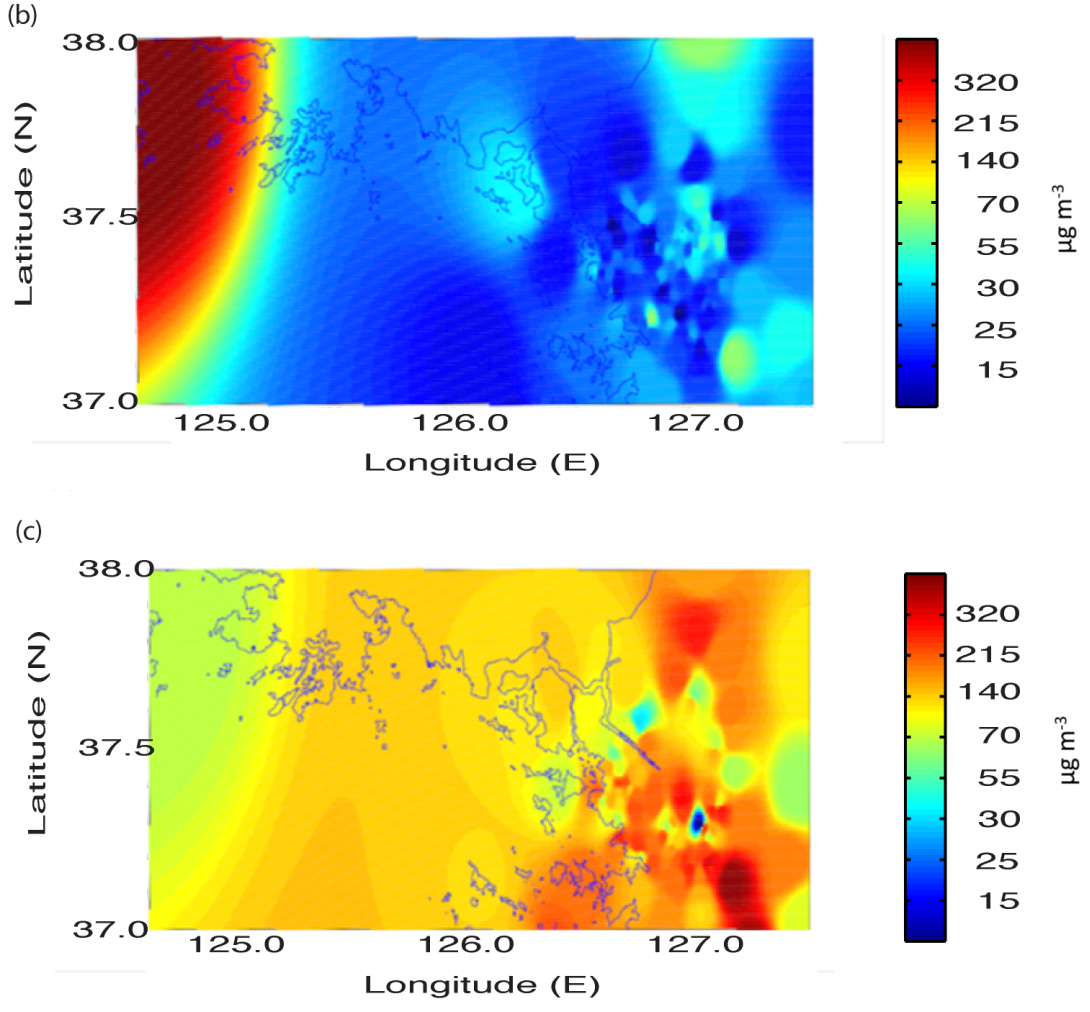

Figures 2b and 2c

https://doi.org/10.5194/acp-2020-1318
Preprint. Discussion started: 11 March 2021

Atmospheric Chemistry and Physics Discussions

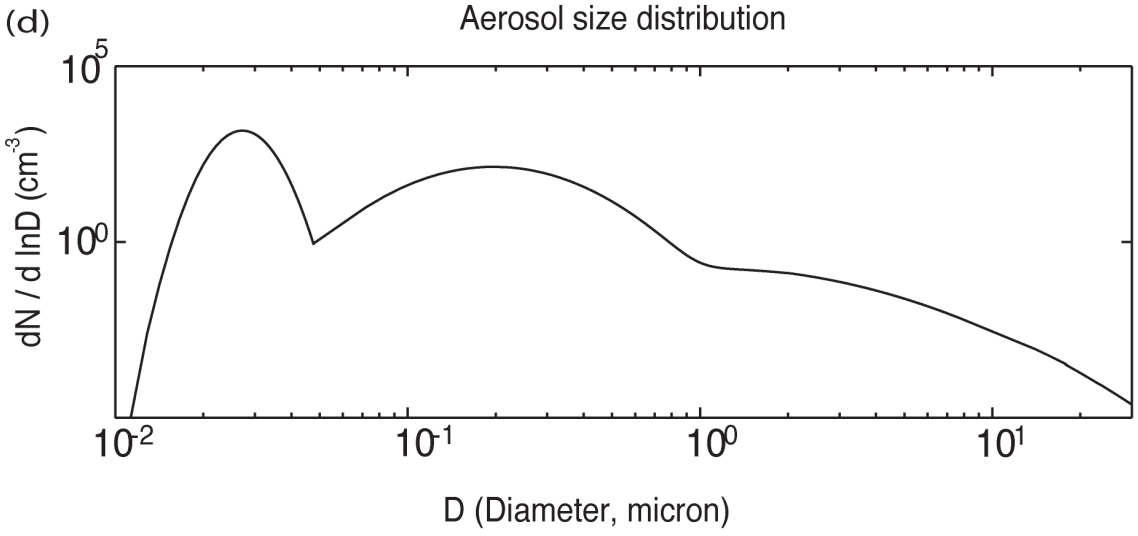

Figure 2d

https://doi.org/10.5194/acp-2020-1318
Preprint. Discussion started: 11 March 2021

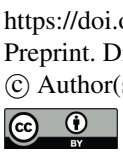

Atmospheric Chemistry and Physics Discussions

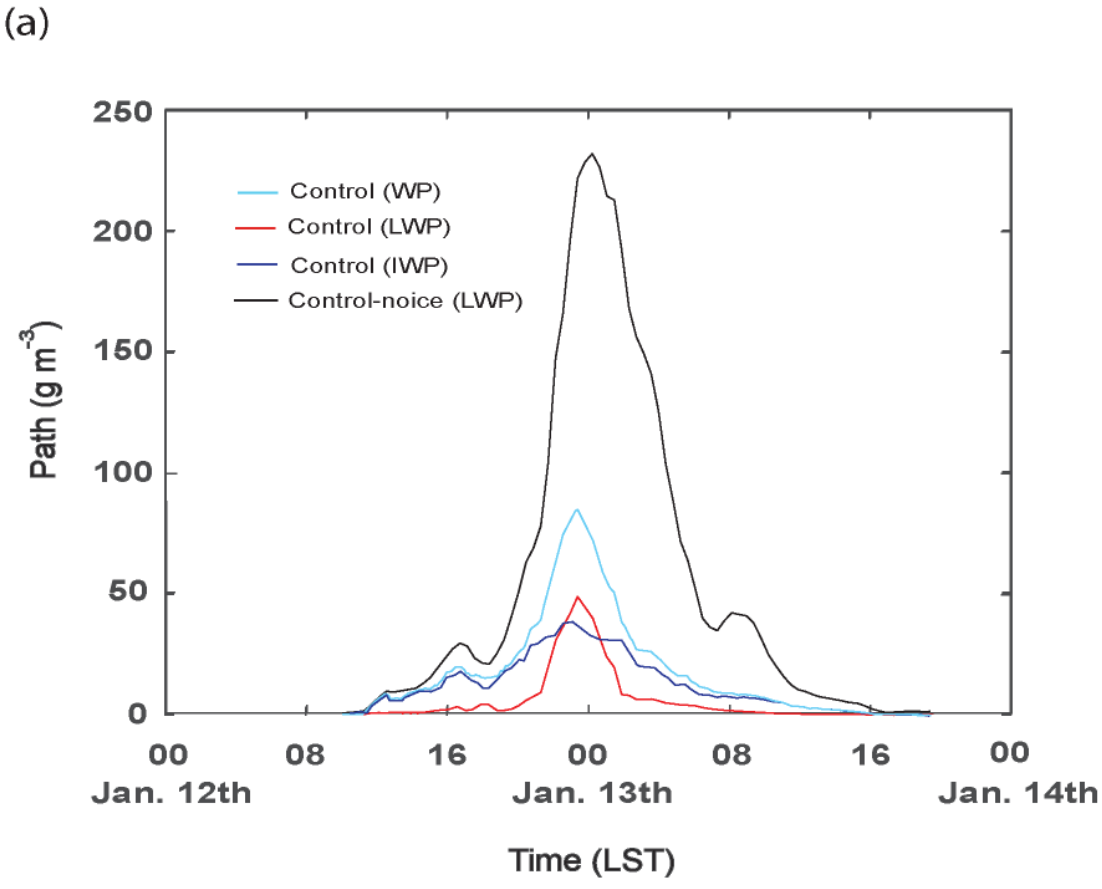

Figure 3a

https://doi.org/10.5194/acp-2020-1318
Preprint. Discussion started: 11 March 2021

Atmospheric Chemistry and Physics Discussions

1334

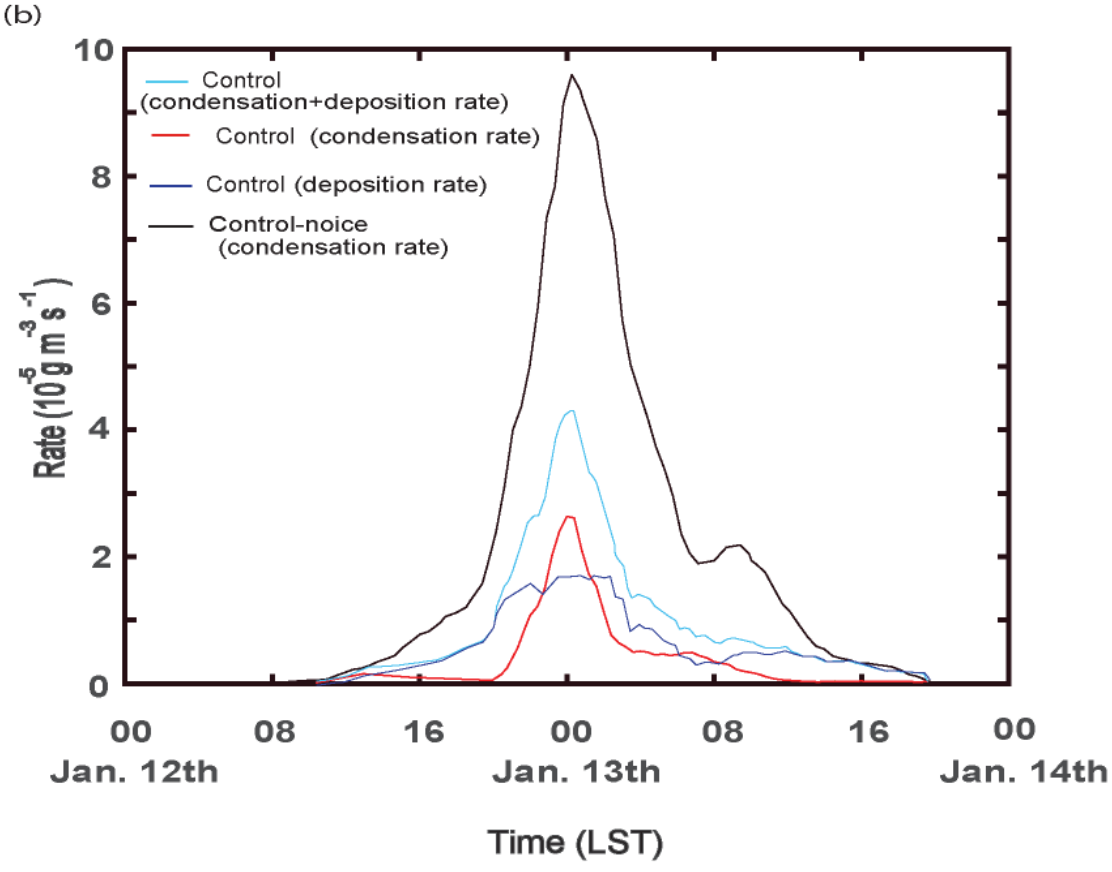

1335
1336
1337 **Figure 3b**
1338
1339
1340
1341
1342
1343
1344
1345
1346
1347
1348

https://doi.org/10.5194/acp-2020-1318
Preprint. Discussion started: 11 March 2021

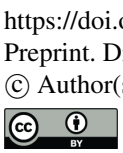

Atmospheric Chemistry and Physics Discussions

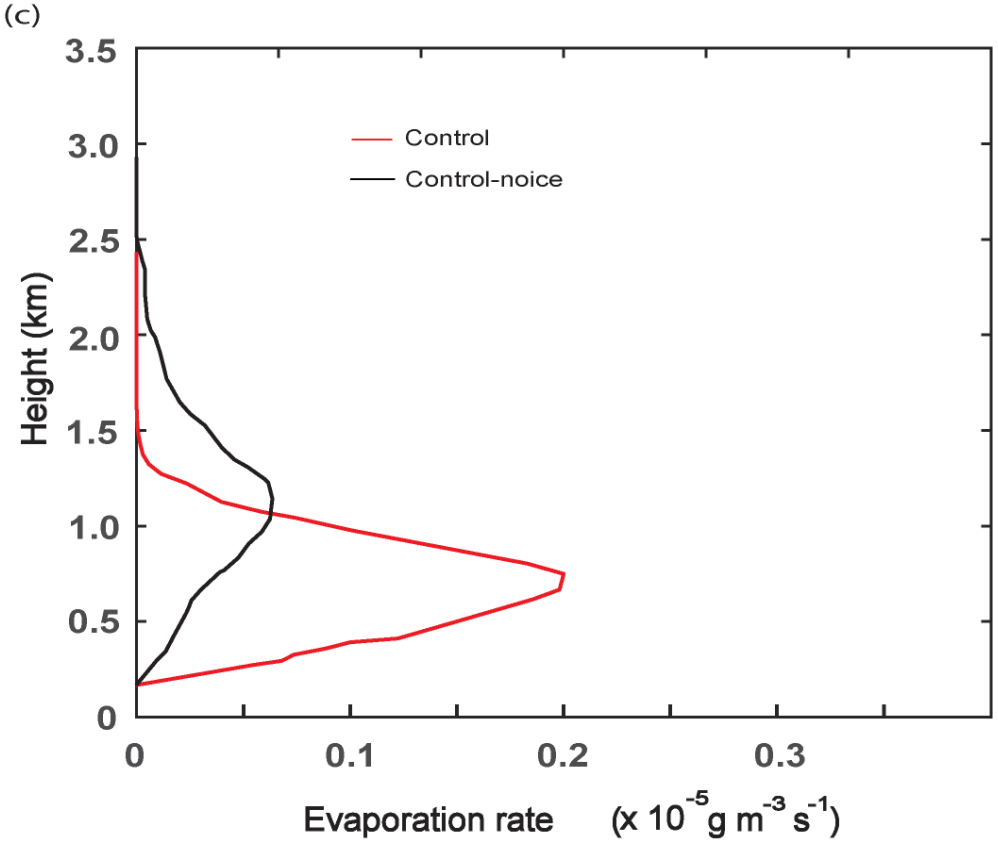

1349
1350
1351 **Figure 3c**
1352
1353
1354

https://doi.org/10.5194/acp-2020-1318
Preprint. Discussion started: 11 March 2021

Atmospheric Chemistry and Physics Discussions

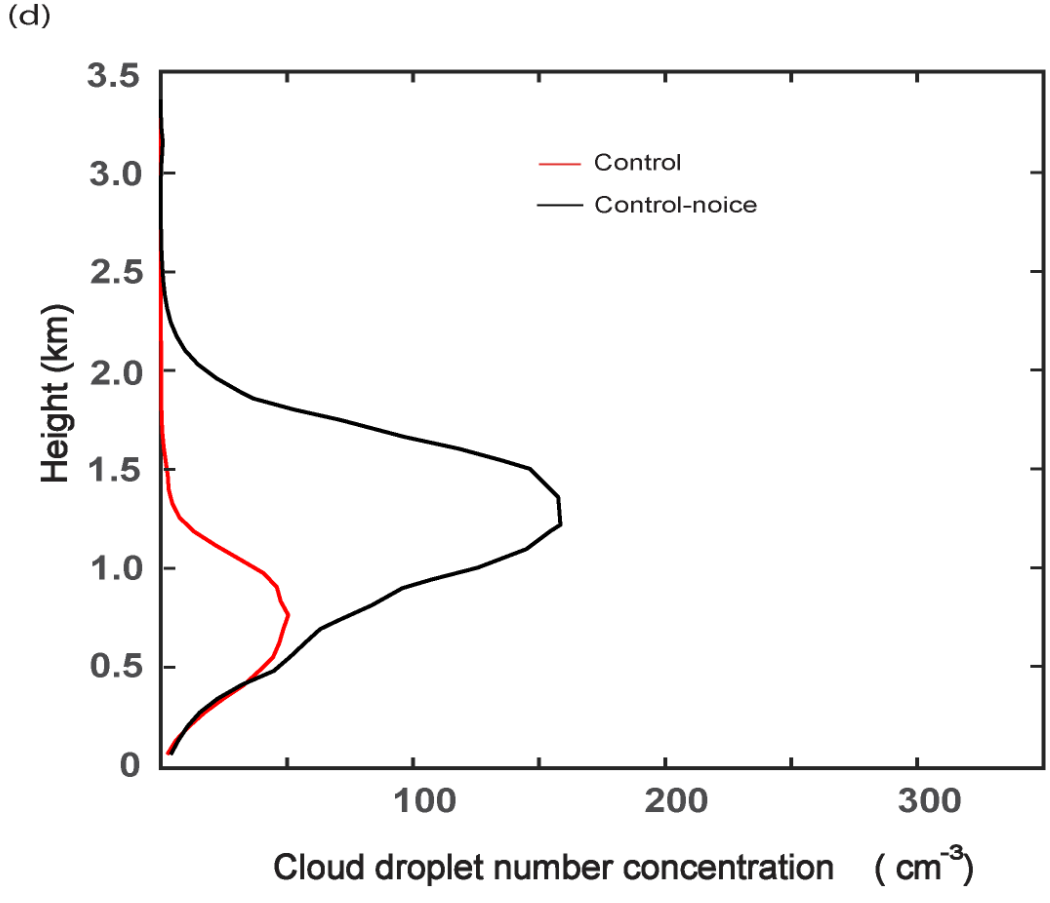

Figure 3d

https://doi.org/10.5194/acp-2020-1318
Preprint. Discussion started: 11 March 2021

Atmospheric Chemistry and Physics Discussions

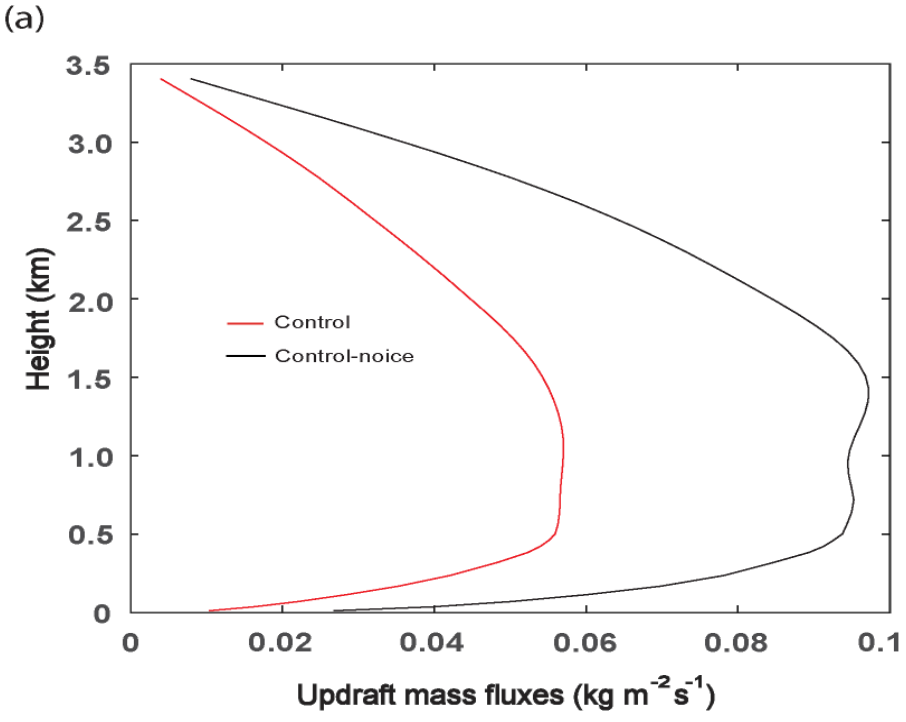

Figure 4a

https://doi.org/10.5194/acp-2020-1318
Preprint. Discussion started: 11 March 2021

Atmospheric Chemistry and Physics Discussions

(b)

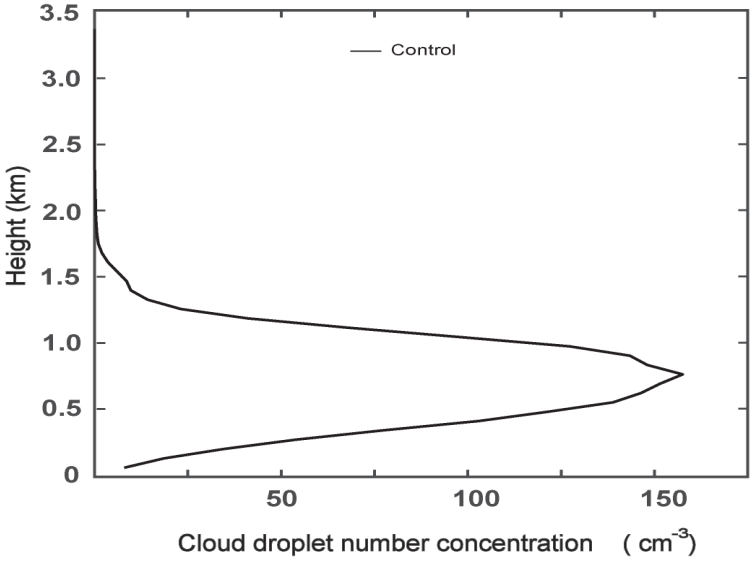

(c)

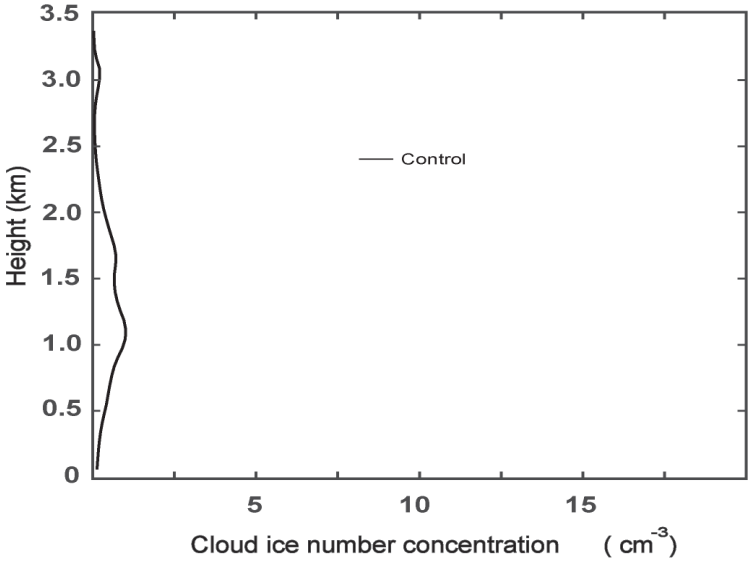

1372

1373 **Figures 4b and 4c**

1374

https://doi.org/10.5194/acp-2020-1318
Preprint. Discussion started: 11 March 2021

Atmospheric Chemistry and Physics Discussions

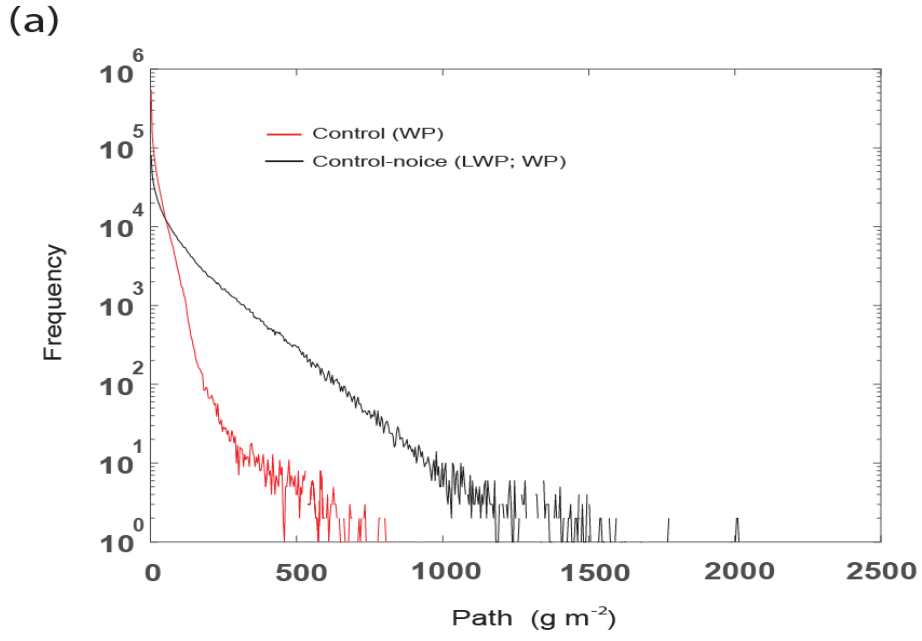

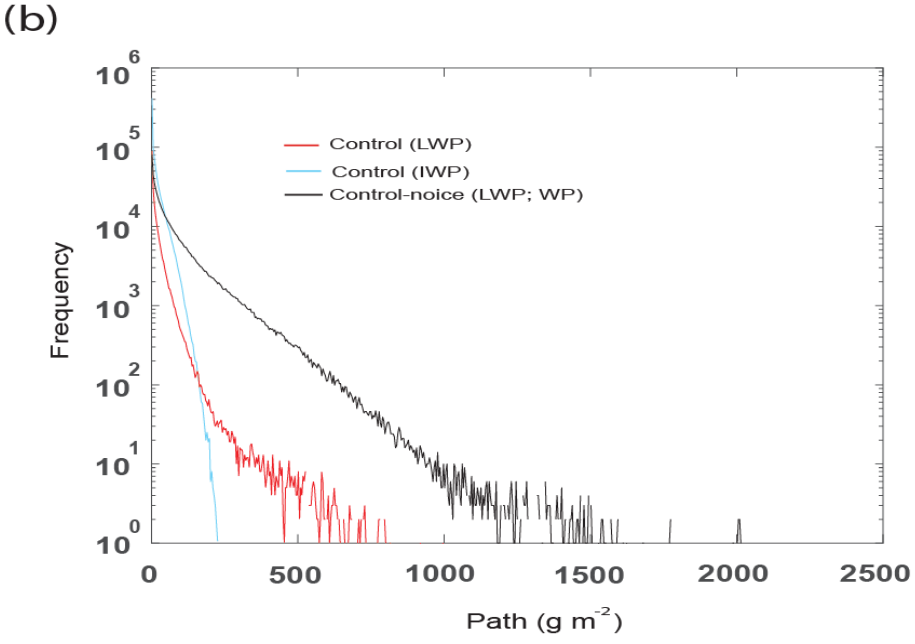

1375

1376 **Figures 5a and 5b**

https://doi.org/10.5194/acp-2020-1318
Preprint. Discussion started: 11 March 2021

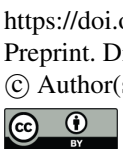

Atmospheric Chemistry and Physics Discussions

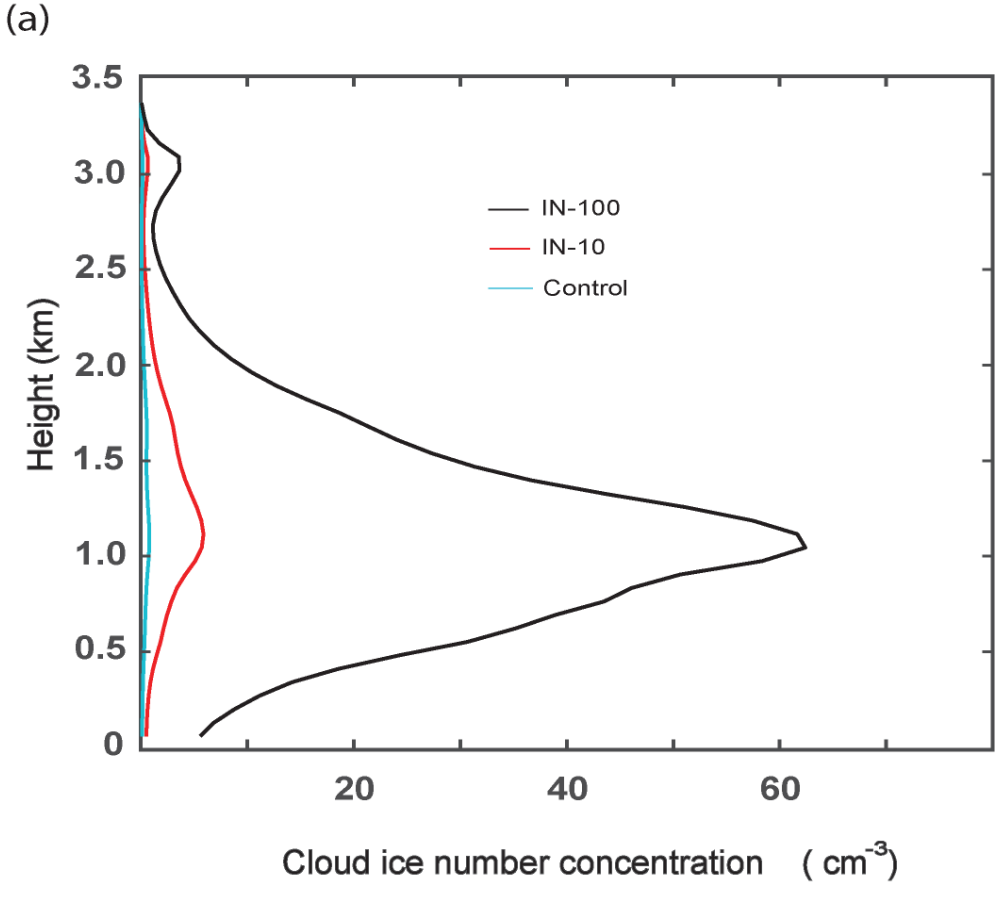

1377

1378 **Figure 6a**

1379

1380

1381

https://doi.org/10.5194/acp-2020-1318
Preprint. Discussion started: 11 March 2021

Atmospheric Chemistry and Physics Discussions

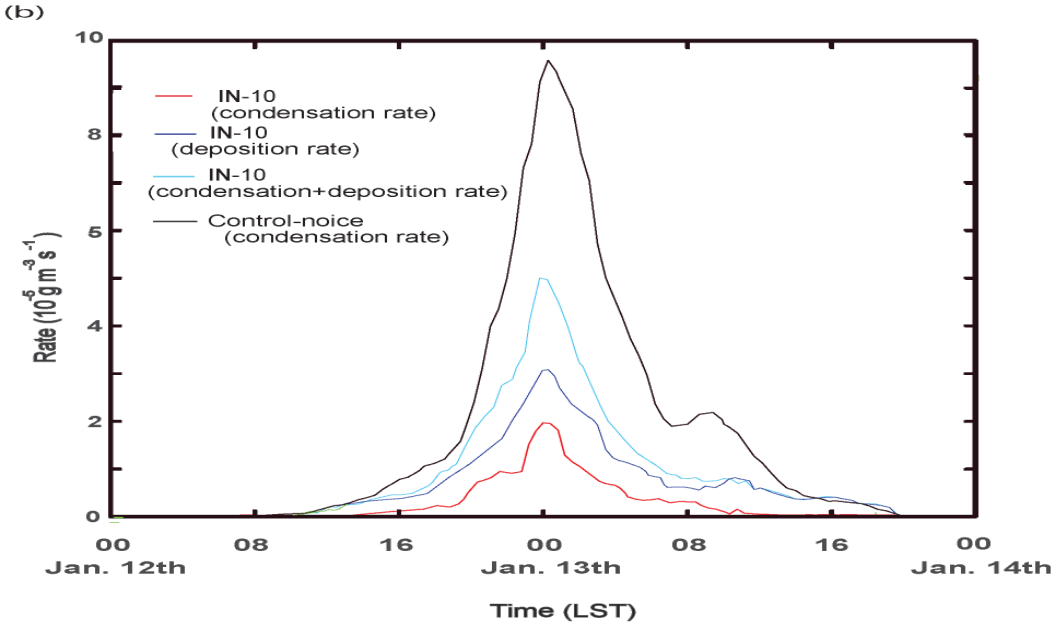

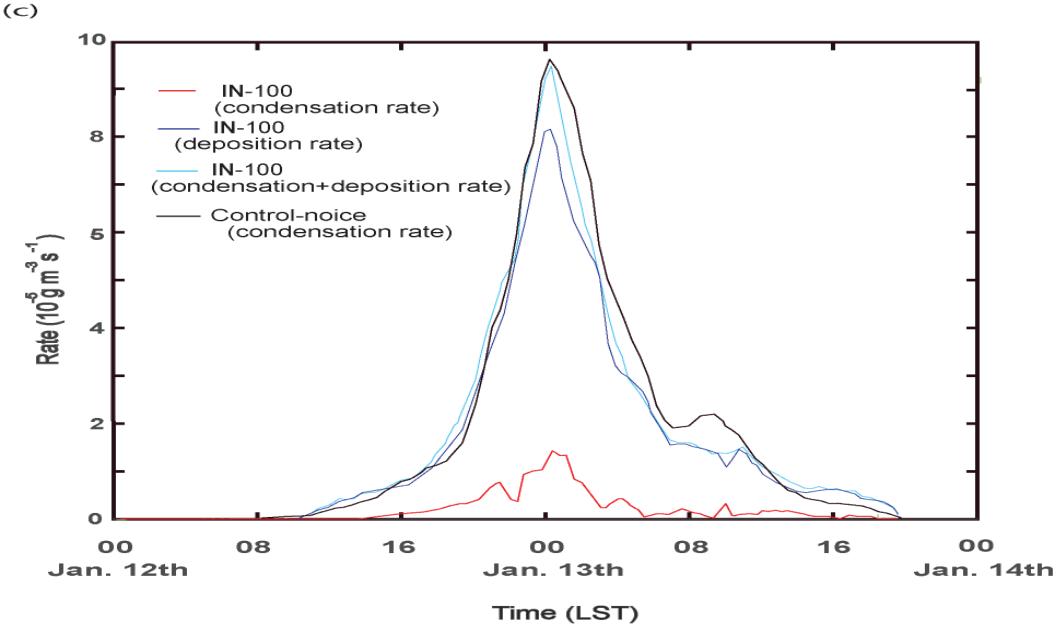

1382

1383 **Figures 6b and 6c**

https://doi.org/10.5194/acp-2020-1318
Preprint. Discussion started: 11 March 2021

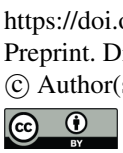

Atmospheric Chemistry and Physics Discussions

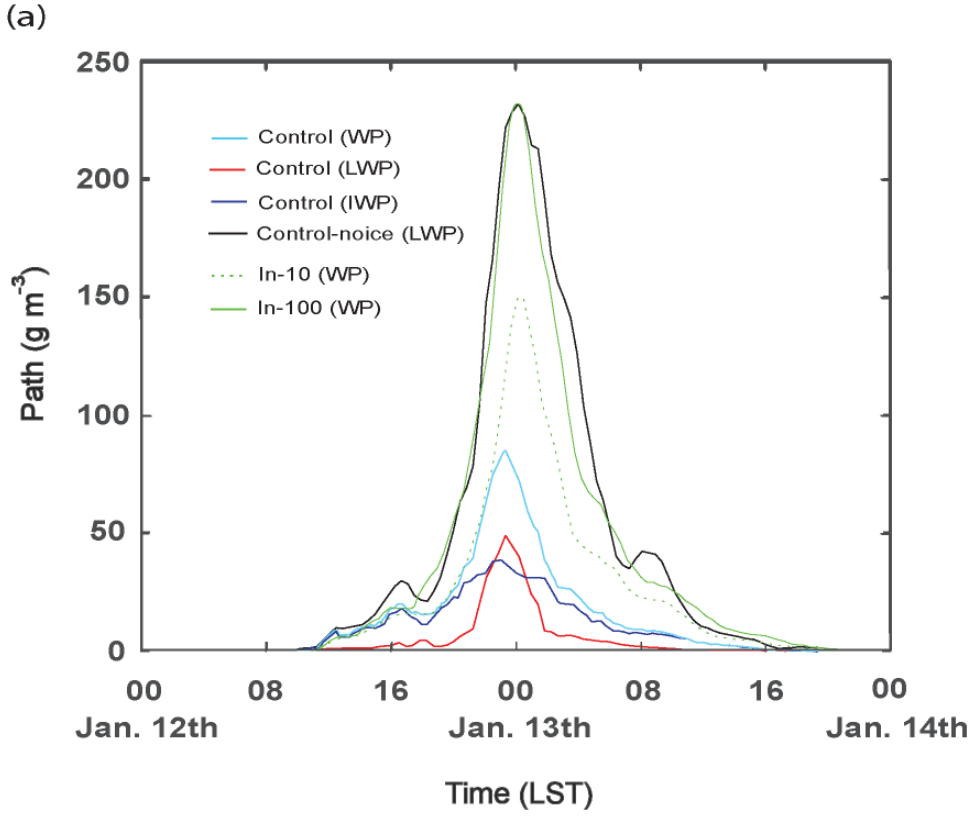

1384

1385 **Figure 7a**

1386

1387

1388

1389

1390

1391

https://doi.org/10.5194/acp-2020-1318
Preprint. Discussion started: 11 March 2021

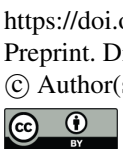

Atmospheric Chemistry and Physics Discussions

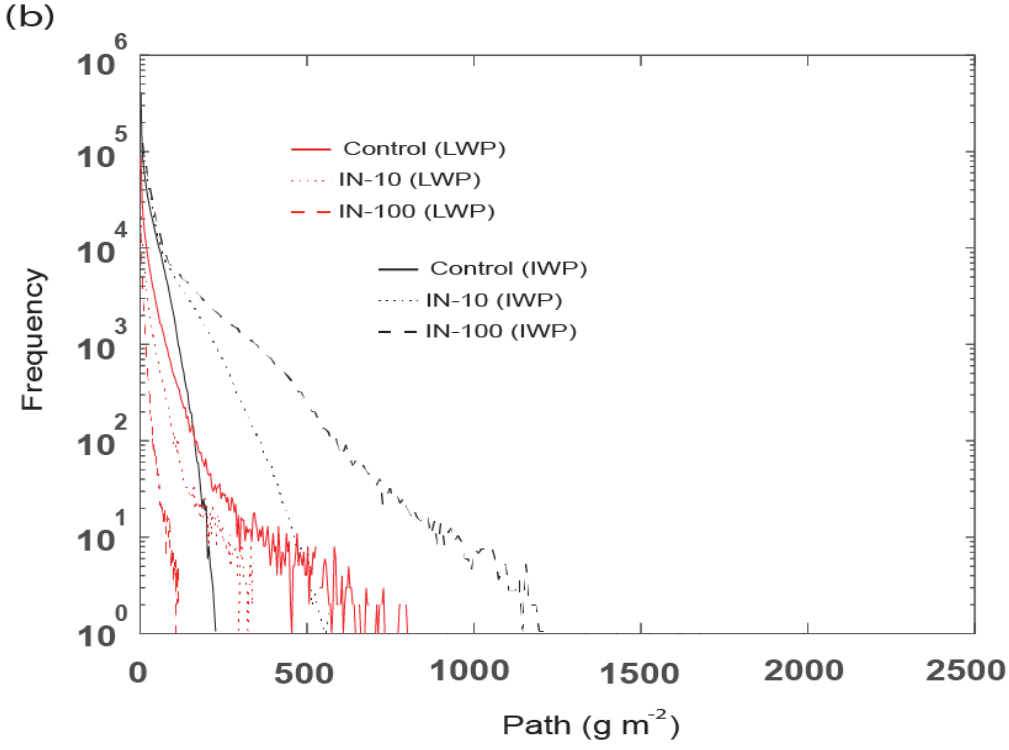

Figure 7b

https://doi.org/10.5194/acp-2020-1318
Preprint. Discussion started: 11 March 2021

Atmospheric Chemistry and Physics Discussions

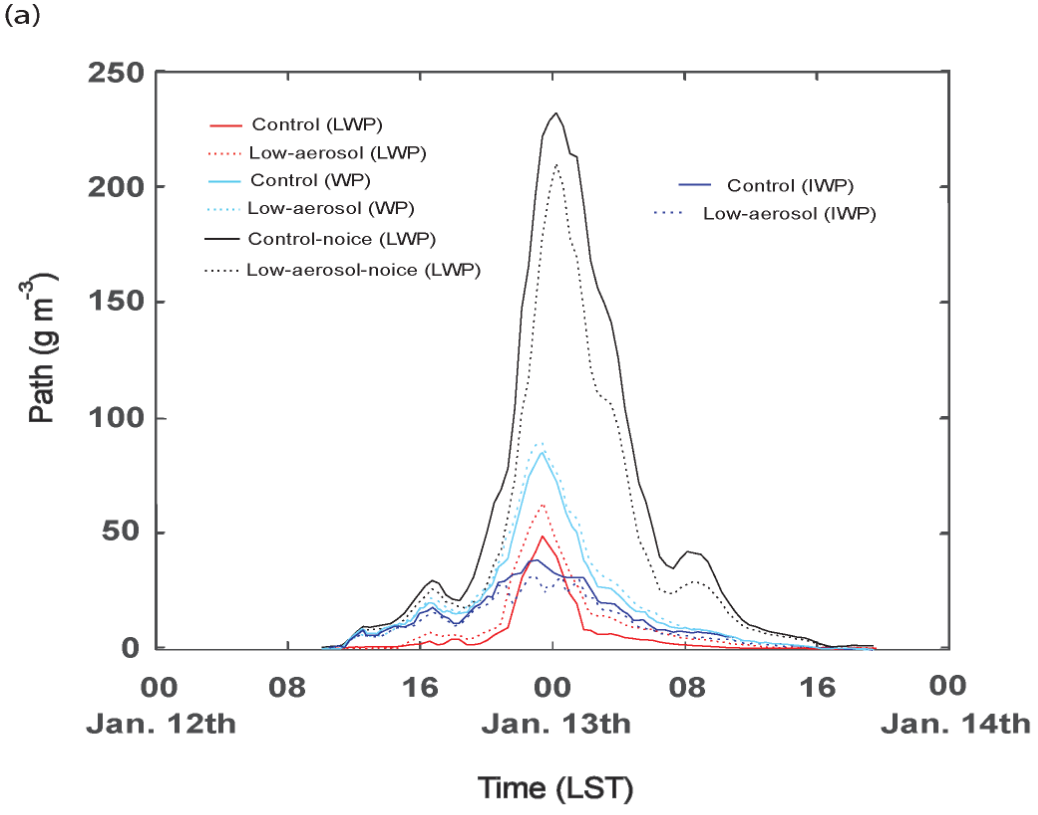

Figure 8a

https://doi.org/10.5194/acp-2020-1318
Preprint. Discussion started: 11 March 2021

Atmospheric Chemistry and Physics Discussions

(b)

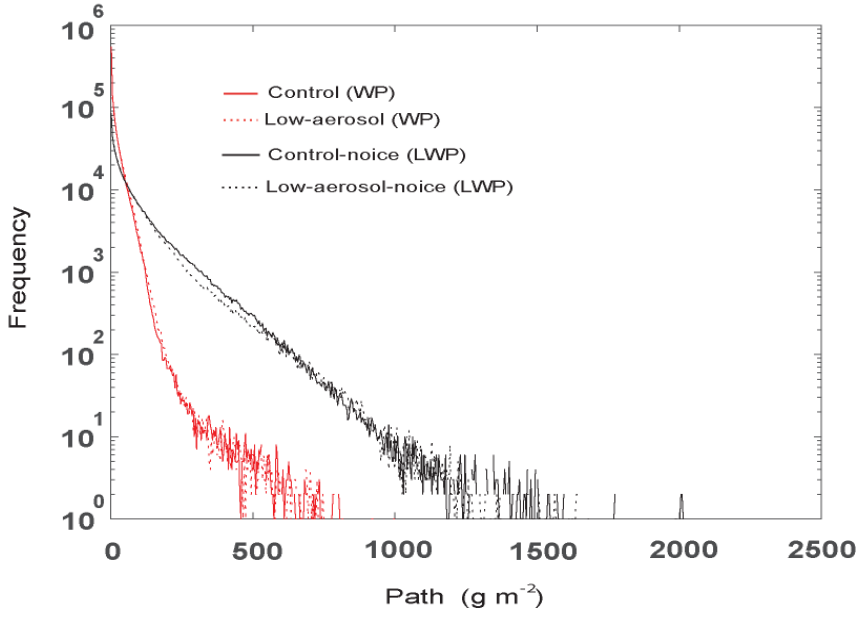

(c)

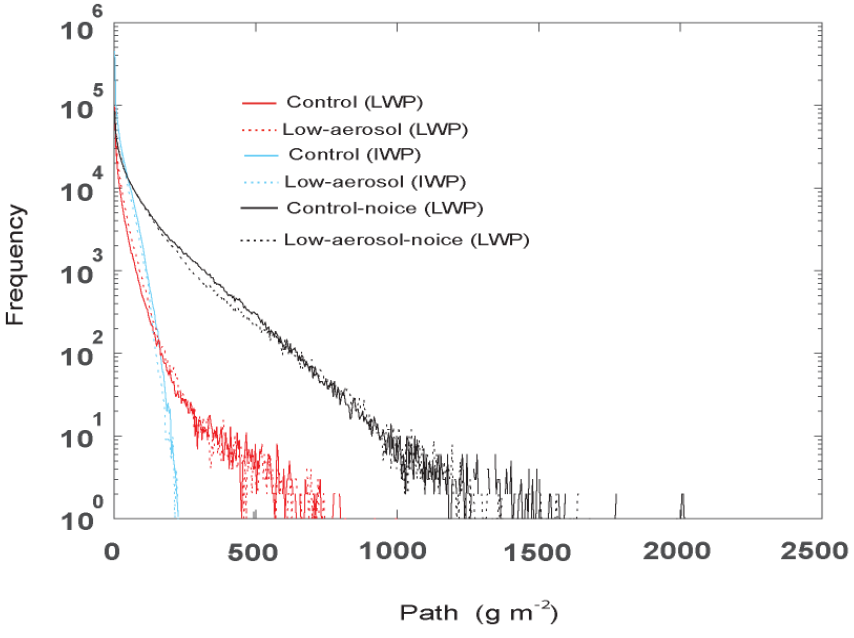

1407

1408 **Figures 8b and 8c**

https://doi.org/10.5194/acp-2020-1318
Preprint. Discussion started: 11 March 2021

Atmospheric Chemistry and Physics Discussions

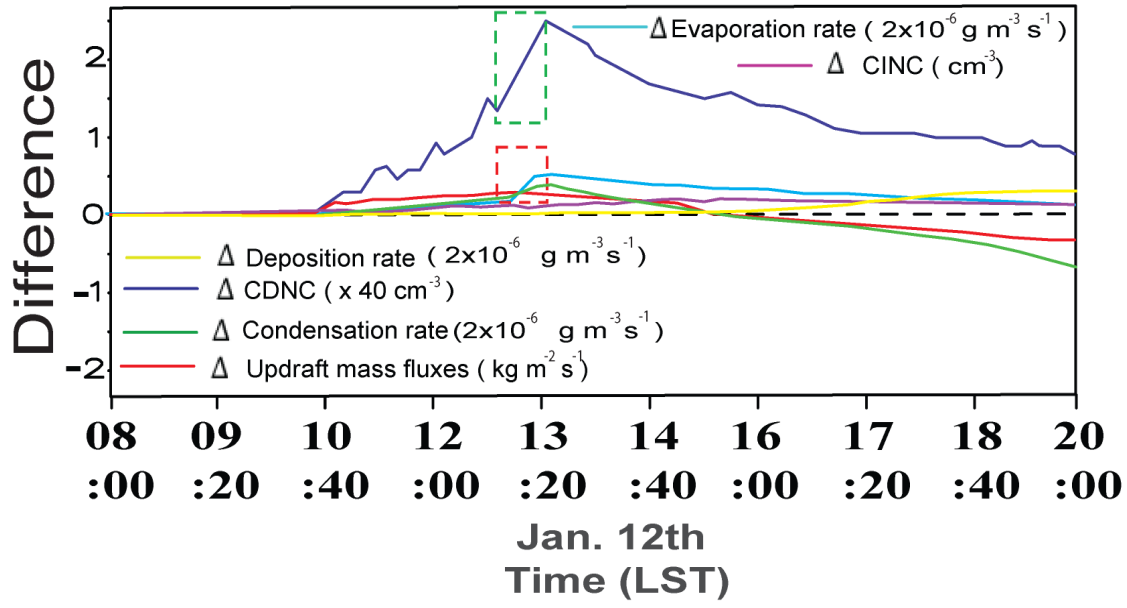

1409

1410 **Figure 9a**

https://doi.org/10.5194/acp-2020-1318
Preprint. Discussion started: 11 March 2021

Atmospheric Chemistry and Physics Discussions

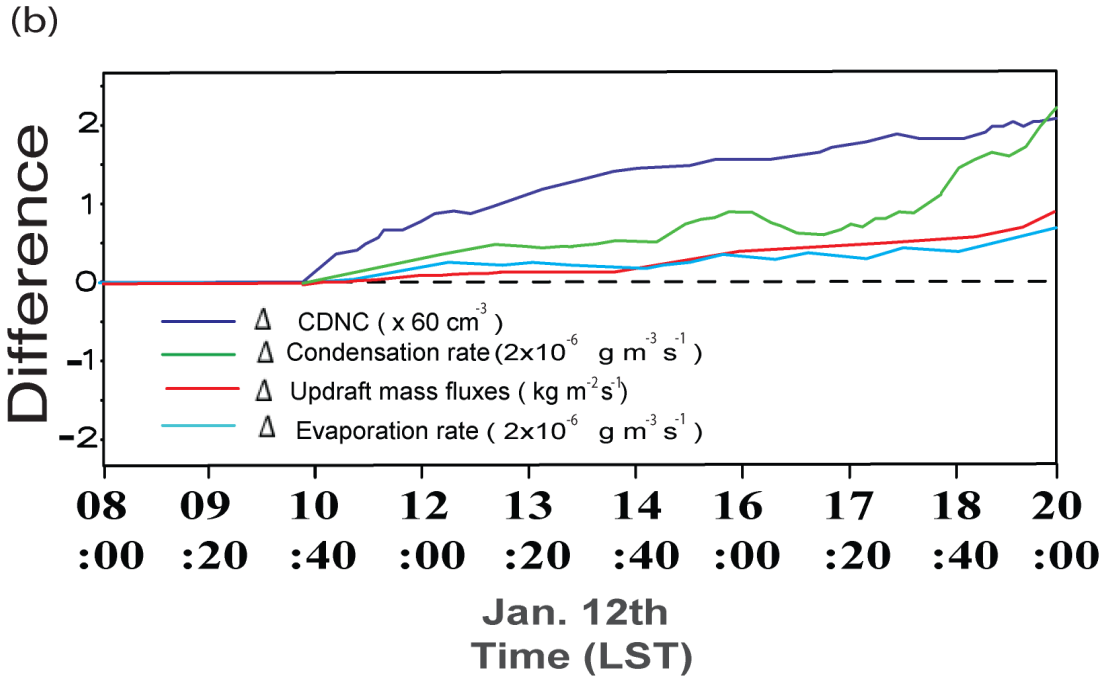

1411

1412 **Figure 9b**

1413

1414

1415

1416

1417

1418

1419

https://doi.org/10.5194/acp-2020-1318
Preprint. Discussion started: 11 March 2021

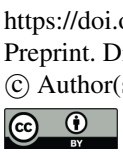

Atmospheric Chemistry and Physics Discussions

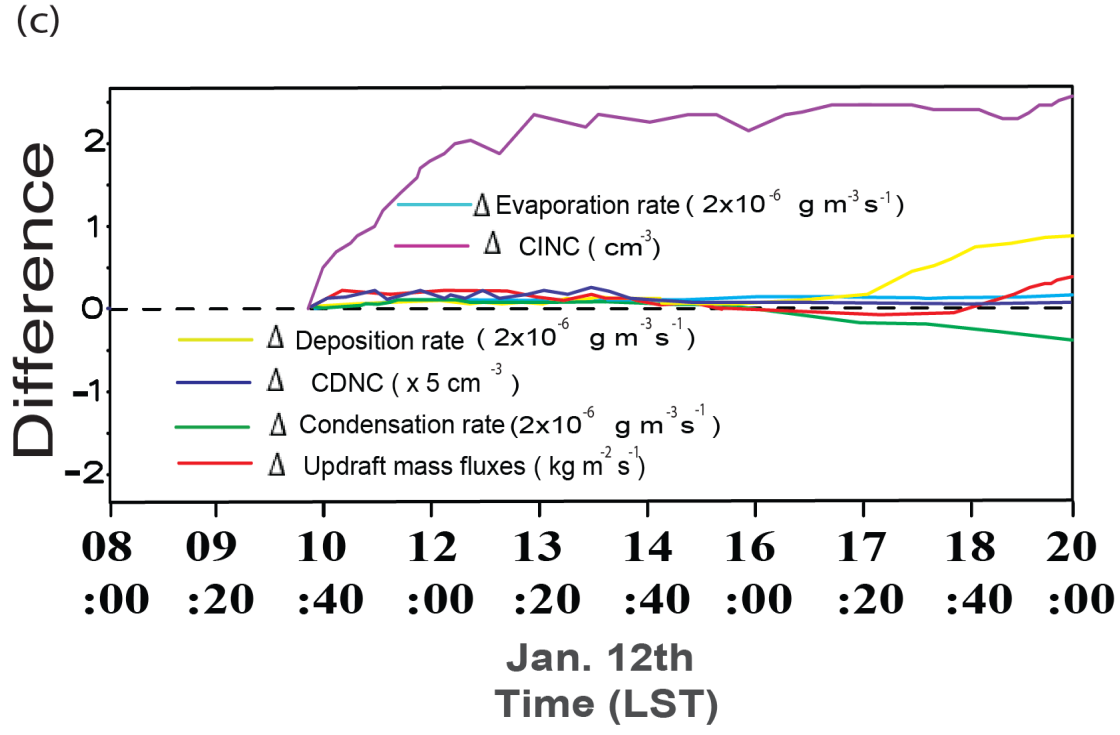

1420

1421 **Figure 9c**

1422

1423

1424

1425

1426

1427

https://doi.org/10.5194/acp-2020-1318
Preprint. Discussion started: 11 March 2021

Atmospheric Chemistry and Physics Discussions

(a)

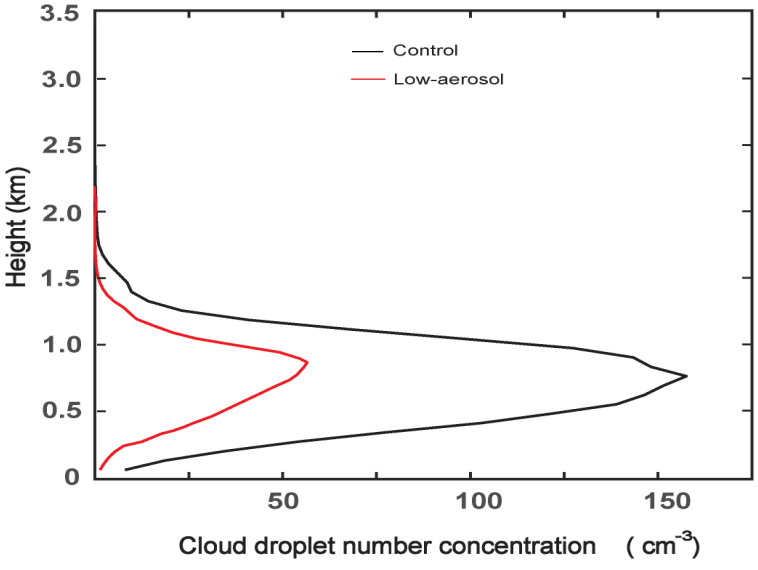

(b)

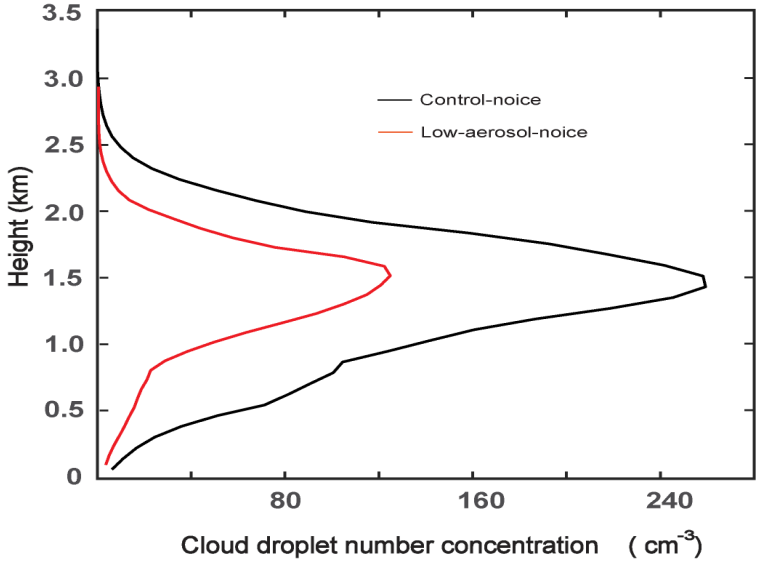

1428

1429 **Figures 10a and 10b**

https://doi.org/10.5194/acp-2020-1318
Preprint. Discussion started: 11 March 2021

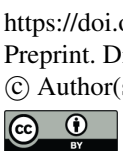

Atmospheric Chemistry and Physics Discussions

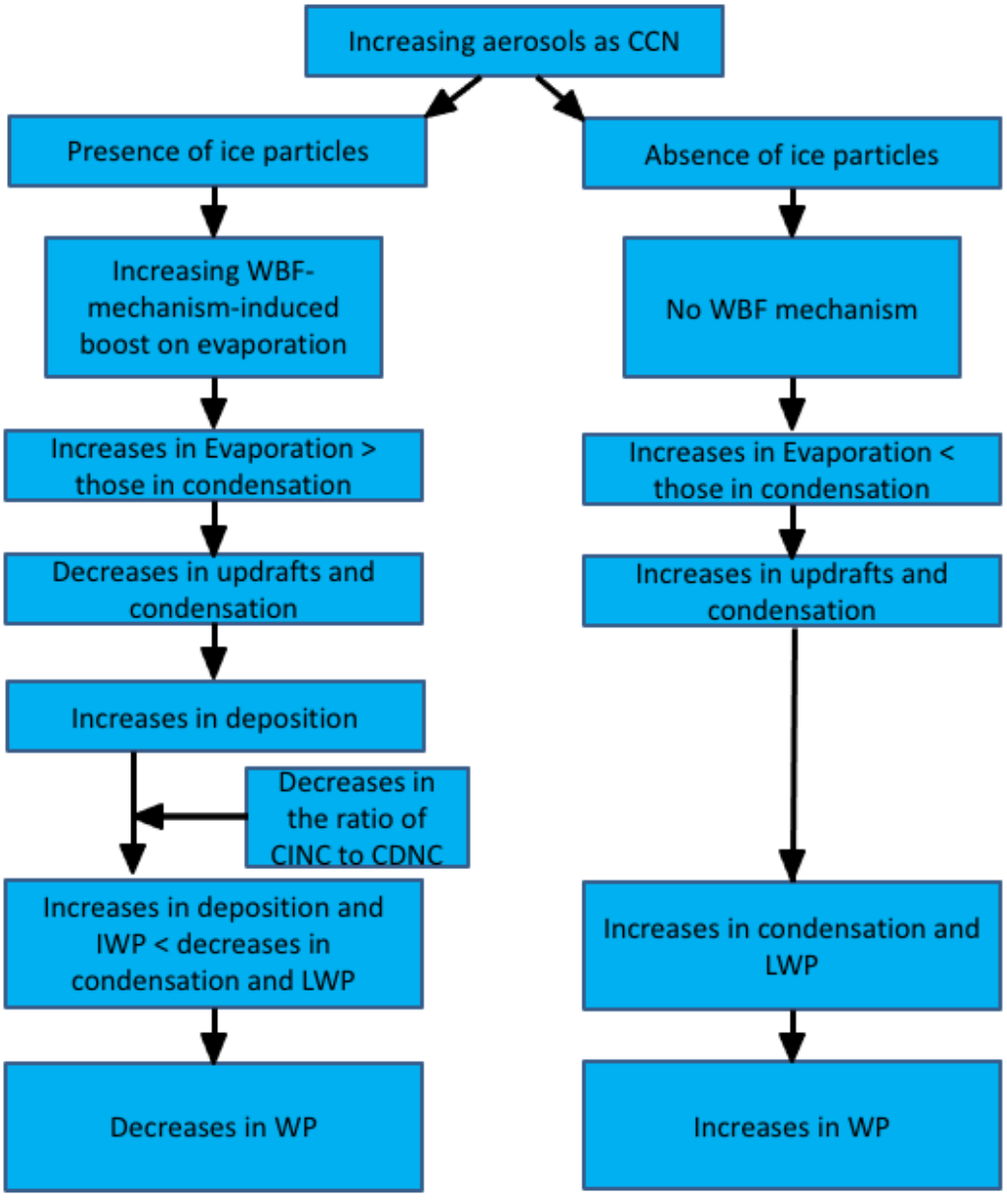

Figure 11

https://doi.org/10.5194/acp-2020-1318
Preprint. Discussion started: 11 March 2021

Atmospheric Chemistry and Physics Discussions

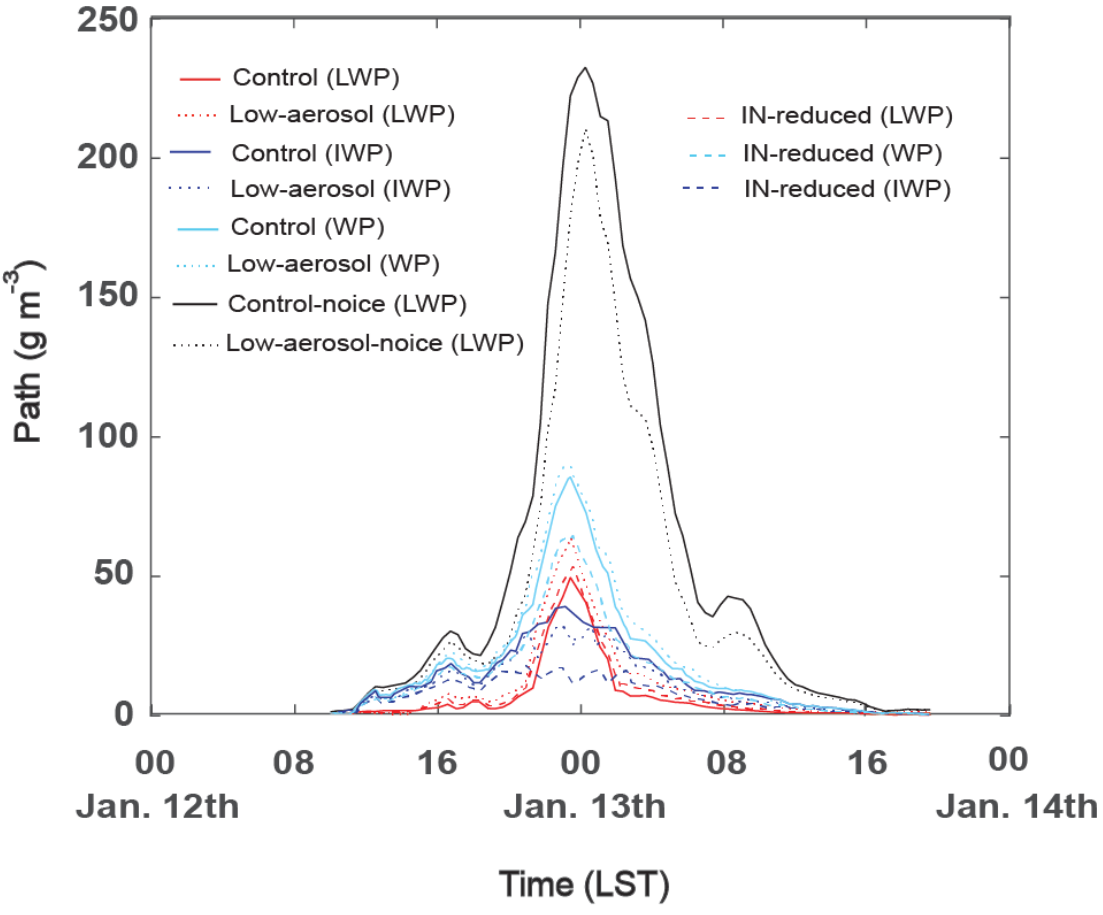

1433

1434 **Figure 12**

1435

1436